

The Capacity of the Multiple Access Channel Under Distributed Scheduling - Order Optimality of Linear Receivers

Joseph Kampeas, Asaf Cohen and Omer Gurewitz
 Department of Communication Systems Engineering
 Ben-Gurion University of the Negev
 Beer-Sheva, 84105, Israel
 Email: {kampeas,coasaf,gurewitz}@bgu.ac.il

Abstract

Consider the problem of a Multiple-Input Multiple-Output (MIMO) Multiple-Access Channel (MAC) at the limit of large number of users. Clearly, in practical scenarios, only a small subset of the users can be scheduled to utilize the channel simultaneously. Thus, a problem of user selection arises. However, since solutions which collect Channel State Information (CSI) from all users and decide on the best subset to transmit in each slot do not scale when the number of users is large, distributed algorithms for user selection are advantageous.

In this paper, we suggest a distributed user selection algorithm, which selects a group of users to transmit without coordinating between all users and without all users sending CSI to the base station. This threshold-based algorithm is analyzed for both Zero-Forcing (ZF) and Minimal Mean Square Error (MMSE) receivers, and its expected capacity in the limit of large number of users is investigated. It is shown that for large number of users it achieves the same scaling laws as the optimal centralized scheme. Multi-stage distributed schemes are also considered and shown to be advantageous in practical scenarios.

1 Introduction

Wireless access networks are the typical last-mile networks connecting multiple users to a high speed backbone. In these networks, a Base Station (BS) serves a large group of users. Traditionally, either the time or the frequency are divided to ensure users do not interfere with each other. Modern coding techniques, however, allow for multiple users to either transmit or receive simultaneously, and be decoded successfully using the appropriate Multiple Access Channel (MAC) codes or Broadcast Channel (BC) codes, respectively.

Nevertheless, consider a BS serving a very large number of users. In practical scenarios, not all users can be served simultaneously, and the problem of user selection or scheduling arises. In the downlink setting, where a BS transmits to a group of users, it is common to assume Channel State Information (CSI) is available at the BS, hence intelligent user

selection can be employed. E.g., the BS can select a subset of the users with both strong channel norms (high SNR) and relatively orthogonal directions (to avoid interference). See Section 2 for a literature survey. Such a selection can exploit the *multi-user diversity* inherent in these models.

In the uplink setting, however, since the users transmit to the BS, it is highly desirable to avoid the process of collecting all information at the BS beforehand, and notifying the users which should transmit. This process is prohibitively complex when the number of users is very large. In fact, this is one of the main reasons why an emerging standard, IEEE 802.11ac, includes Multi-User Multiple Input Multiple Output (MU-MIMO) only at the downlink [10]. That is, the allegedly complex process of selecting a subset of users in the uplink is refrained from. Hence, efficient and distributed algorithms for selecting the appropriate group of users are desirable. This way, there is hope to harness the benefits of multi-user diversity without the need to collect CSI from all users. In this paper, we show that this is indeed possible, by showing the order-optimality of distributed algorithms.

Main Contribution

We consider a MIMO MAC channel with r receiving antennas and $K \gg r$ users. We suggest distributed algorithms for selecting a group of users to transmit in each slot. In the first, a threshold value for the norm of the channel vector is set, and only users above the threshold transmit. Hence, there is no need to collect CSI from all users. Nor is any cooperation required. In the second, an iterative process is suggested, where *multiple thresholds* are set on the norms of the *projections of the channel vectors* on the spaces of previously selected users. In this case, CSI is shared, but *only among the selected group*.

An analysis of the resulting sum capacity in the limit of large K and the respective scaling laws are given for both Zero-Forcing (ZF) and Minimal Mean Square Error (MMSE) receivers. This analysis employs recent tools from both Point Process approximation and asymptotic random matrix theory, that to the best of our knowledge, were not used in this setting before. Via this analysis, the simple distributed, threshold based algorithm, is shown to achieve the optimal scaling laws. Consequently, the benefit compared to traditional (centralized) techniques is demonstrated both analytically and via simulation results.

The rest of this paper is organized as follows: Section 2 includes the most relevant related work. Section 3 includes the required preliminary material. Section 4 introduces the distributed algorithm, gives its analysis and scaling law under ZF decoding. Section 5 gives an improved, multi-stage algorithm, which, while only semi-distributed (as it requires messaging between the selected users), gives better performance for a small number of users. Section 6 gives the analysis under an MMSE receiver. While conceptually similar, this analysis is the more technically challenging. Section 7 gives the previously omitted proofs. Section 8 concludes the paper.

2 Related Work

The essence of multi-user diversity was introduced in [11], where selecting the strongest user in each time slot was first suggested. The work was followed by numerous scheduling algorithms for various scenarios. We list here only the most relevant.

In [12], the authors considered the impact of multi-user diversity on the MIMO downlink channel (BC). Assuming channel state information at the BS, the authors used order statistics to evaluate the effective SNR when scheduling the strongest user in each slot. However, *only one user was scheduled* in each slot, and the results were given in terms of the K -fold statistics, without an extreme value analysis for large K .

In [13], a similar downlink model was considered, however, when users are scheduled simultaneously. The authors considered Zero-Forcing Beamforming (ZFBF), and suggested a greedy algorithm to schedule the strongest and most orthogonal users. Additional scheduling algorithms for downlink communication were given in [14, 15, 16, 17]. In fact, in the downlink scenario, it was shown later that ZFBF and optimal user selection can indeed achieve the Dirty Paper Coding (DPC) region [18], and is hence optimal in the Gaussian case [19]. Additional surveys and scaling laws can be found in [20, 21, 22].

A closely related scheme, yet still for the downlink model, was suggested in [23]. Using Block Diagonalization (BD), a capacity-based greedy algorithm was suggested, in which first the strongest user is scheduled, and then additional users are added, one by one, based on their marginal contribution to the total capacity. In the same context, [24] considered the special case of two transmit antennas and one receive antenna per user, and showed that a greedy, two-stage algorithm, which first selects the strongest user and then the second to form the best pair is asymptotically optimal. In the context of heterogeneous users, [25] proposed a scheduling scheme which selects a small subset of the users with favorable channel characteristics.

The above works focus on the downlink setting. In this scenario, it is reasonable to assume that at least some information is available at the BS, and a centralized decision can be made. In the uplink (MAC) model, however, if one wishes to select a group of users without centralized processing at the BS, distributed algorithms are required. In this paper, we suggest both a single-stage distributed algorithm, and a multi-stage semi-distributed one for the uplink scenario, and, in addition, analyze their sum capacity in the limit of large number of users and give the resulting scaling laws.

A pioneering study of the uplink model was done in [26, 27], where a decentralized MAC protocol for Orthogonal Frequency Division Multiple Access (OFDMA) channels was suggested. In this scheme, each user estimates the channel gain and compares it to a threshold. Only above-the-threshold users can transmit. [28] extended the scheme to a multi-channel setup, where each user competes on m channels. In [9], the authors used a similar approach for power allocation in the multi-channel setup, and suggested an algorithm that asymptotically achieves the optimal water filling solution. However, the works above do not consider a *MIMO setting*, nor do they consider the interaction within a group of users, when all are scheduled to use *the same resources*. Space-time coding for fading multi-antenna MAC was considered in [8]. The focus therein, however, was on joint code design for a given point in the rate region and the resulting error probability, rather than user scheduling and its resulting capacity.

Recently, we proposed a Point Process approximation which facilitates the analysis of various distributed threshold-based scheduling algorithms in the non-homogeneous scenario [29, 30]. This work, however, assumed only a single user can be successfully decoded in each time slot. A key contribution of the current work is the non-trivial extension of the work in [29] to truly multiple-access protocols, where several users transmit simultaneously and should be decoded successfully, hence the questions that arise are how to distributively

select a good subset of users to transmit and what the mutual influence between the users in the selected group is. For example, a closely related work is [31]. Therein, various decoding procedures were discussed, and the corresponding best user selection *for the uplink setting* was given. However, while reinforcing the necessity of proper user selection, the work in [31] considered only the scenario where *one user* can access the radio channel at a given time.

As for more complex topologies, spatial diversity in the context of multiple relays was considered in [32]. Therein, communication between a source and a destination is done through a group of relays. However, unlike conventional relay schemes, only the relays with the *strongest received signal* decode the message and cooperate via space time coding to successfully relay it to the destination. An asymptotically optimal scheme for multiple base stations (with joint optimization) was given in [33].

Extreme Value Theory (EVT) is a key tool in proving capacity results under scheduling and multi-user diversity. In [34], the authors suggested a sub-carrier assignment algorithm, and used order statistics to derive an expression for the resulting link outage probability. In [35], the authors used EVT to derive the scaling laws for scheduling systems using beamforming and linear combining. [36] analyzed the scaling laws of base station scheduling, and showed that by scheduling the strongest among K stations one can gain a factor of $O(\sqrt{2 \log K})$ in the expected capacity (compared to random or Round-Robin scheduling).

3 Preliminaries

In this section, we describe the system model and relevant results which will be used throughout this paper.

3.1 System Model

Throughout this paper, random matrices and random vectors are denoted in bold upper-case and bold lower-case letters, respectively. We consider a multiple-access model with K users, each with a single transmit antenna. The BS is equipped with r receiving antennas. When k users utilize the channel simultaneously, the received signal at the base station can be described as:

$$\mathbf{y} = \sum_{i=1}^k \mathbf{h}_i \mathbf{x}_i + \mathbf{w}, \quad (1)$$

where $\mathbf{x}_i \in \mathbb{C}$ is the transmitted signal (scalar). \mathbf{x}_i is constrained in its total power to P , i.e., $E[\mathbf{x}_i^\dagger \mathbf{x}_i] \leq P$. However, in most cases, we will assume a *constant* power constraint P . $\mathbf{w} \in \mathbb{C}^r$ denotes the uncorrelated Gaussian noise. $\mathbf{h}_i \in \mathbb{C}^{r \times 1}$ is a complex random Gaussian channel vector. When all users are identically and independently distributed, it is common to assume that all entries of \mathbf{h}_i are independent and have zero mean and variance $1/2$ imaginary and real parts, for all users. We assume that the channel is memoryless, that is, for each channel use (slot), independent realizations of $\{\mathbf{h}_i\}_{i=1}^K$ are drawn. Furthermore, we assume full CSI is available at the transmitter. That is, \mathbf{h}_i is known to the i th user. This can be accomplished by sending a pilot signal from each of the r antennas at the base station.

3.2 Capacity and Multi-User Diversity Via EVT

EVT is a key tool in evaluating the capacity under scheduling in multi-user systems. We review here the most relevant result. Moreover, we develop new normalizing constants for the problem at hand (EVT for the χ^2 distribution), which will later aid at speeding up convergence results.

The capacity obtained by letting an arbitrary user i utilize the channel is given by $C = \log(1 + P\|\mathbf{h}_i\|^2)$. However, as mentioned, it is beneficial to schedule the strongest user in each slot. Denote by $\mathbf{h}_{(1)}$ the received channel vector with the largest norm. Scheduling the strongest user clearly results in $C = \log(1 + P\|\mathbf{h}_{(1)}\|^2)$, while letting a *group of r orthogonal users*, with the largest channel gains to utilize an uplink channel, results in a sum-rate that has the following upper bound:

$$C \leq r \log(1 + P\|\mathbf{h}_{(1)}\|^2).$$

Remark 1. *For the downlink channel, the sum-rate upper bound has the form [25]*

$$C \leq r \log\left(1 + \frac{P}{r}\|\mathbf{h}_{(1)}\|^2\right).$$

The difference between the uplink to the downlink originates in the power constraint applied to the transmitter. That is, in the downstream, when transmitting to a group of receivers, each receiver gets a share of the available power, while in the upstream, there is a group of transmitters that transmit to a single receiver. It should be noted that usually the power constraint P for the downlink and uplink are not equal, since the base station has a strong and steady power supply, whereas the user has a limited battery power supply.

As the sum rate is mainly influenced by the channel vectors' gains and directions, our goal is to explore this behavior for large number of users. Specifically, we first wish to explore the behavior of the maximal gain. Since the entries of \mathbf{h} are complex Gaussian, the channel's gain follows a χ^2 distribution with $2r$ degrees of freedom, denoted χ_{2r}^2 . We utilize the following EVT theorem.

Theorem 1 ([37, 38, 39]). *Let $\mathbf{x}_1, \dots, \mathbf{x}_n$ be a sequence of i.i.d. random variables with distribution $F(x)$, and let $\mathbf{M}_n = \max(\mathbf{x}_1, \dots, \mathbf{x}_n)$. If there exists a sequence of normalizing constants $a_n > 0$ and b_n such that as $n \rightarrow \infty$,*

$$\Pr(\mathbf{M}_n \leq a_n x + b_n) \xrightarrow{i.d.} G(x)$$

for some non-degenerate distribution G , then G is of the generalized extreme value (GEV) distribution type

$$G(x) = \exp\left\{-(1 + \xi x)^{-1/\xi}\right\}$$

and we say that $F(x)$ is in the domain of attraction of G , where ξ is the shape parameter, determined by the ancestor distribution $F(x)$.

The normalizing constants and the shape parameter of the GEV can be obtained as follows. Let $h(x)$ be the reciprocal hazard function

$$h(x) = \frac{1 - F(x)}{f(x)} \text{ for } x_F \leq x \leq x^F,$$

where $x_F = \inf\{x : F(x) > 0\}$ and $x^F = \sup\{x : F(x) < 1\}$ are the lower and upper endpoints of the ancestor distribution, respectively. The shape parameter ξ is obtained as the following limit [37, 38]:

$$\xi = \lim_{x \rightarrow x^F} \frac{d}{dx} h(x).$$

When $\{\mathbf{x}_n\}$ is a sequence of i.i.d. χ_{2r}^2 variables, the asymptotic distribution of \mathbf{M}_n is a Gumbel distribution [39, pp. 156]. Specifically,

$$\Pr(\mathbf{M}_n \leq a_n x + b_n) \longrightarrow e^{-e^{-x}},$$

where

$$a_n = 2, \tag{2}$$

$$b_n = 2(\log n + (r-1)\log \log n - \log \Gamma(r)) + o(1), \tag{3}$$

and $\Gamma(r) = \int_0^\infty t^{r-1} e^{-t} dt$ is the Gamma function. In the sequel, we will also use the upper incomplete Gamma function, $\Gamma(r, x) = \int_x^\infty t^{r-1} e^{-t} dt$.

However, for i.i.d. χ_{2r}^2 random variables, the convergence of the maxima to the Gumbel distribution using the above normalizing constants is quite slow. That is, the approximation of the maximal value will not be tight for moderate values of $r, n \in \mathbb{N}$. Hence, a more appropriate set of normalizing constants for the χ_{2r}^2 distribution, which takes into account both r and n should be derived. Letting b_n to be the $1 - 1/n$ quantile, i.e., $1 - F_{\chi^2}(b_n) = 1/n$, and choosing $a_n = h(b_n)$ [37, 38], we have the following.

Claim 1. *For the χ_{2r}^2 -distribution, the following normalizing constants apply.*

$$a_{\{n,r\}} = \frac{2}{n} \Gamma(r) \exp \left\{ Q^{-1} \left(r, \frac{1}{n} \right) \right\} Q^{-1} \left(r, \frac{1}{n} \right)^{1-r} \tag{4}$$

$$b_{\{n,r\}} = 2Q^{-1} \left(r, \frac{1}{n} \right) + o(a_{\{n,r\}}), \tag{5}$$

where $Q^{-1} \left(r, \frac{1}{n} \right)$ is the inverse of the regularized upper incomplete gamma function, that is, $Q(r, x) = \frac{\Gamma(r, x)}{\Gamma(r)}$, and the inverse is defined with respect to x .

Proof. The χ^2 distribution is a special case of the gamma distribution. I.e., if $\mathbf{x} \sim \chi_{2r}^2$ then $\mathbf{x} \sim \Gamma(r, \beta = 2)$, where $\Gamma(r, \beta = 2)$ is the Gamma distribution with shape parameter r and rate parameter β . Accordingly, for the $b_{\{n,r\}}$ constant we consider the $1 - 1/n$ quantile of the Gamma distribution, which can be obtained by using the inverse of the regularized upper incomplete gamma function. In particular, $b_{\{n,r\}} = \beta Q^{-1} \left(r, \frac{1}{n} \right)$ yields the $1 - 1/n$ quantile of the Gamma distribution. To attain the $a_{\{n,r\}}$ constant, let us examine the hazard function $h(x)$ of the Gamma distribution.

$$\begin{aligned} h(x/\beta) &= \frac{1 - F_\Gamma(x/\beta)}{f_\Gamma(x/\beta)} \\ &= \beta e^{x/\beta} (x/\beta)^{1-r} \Gamma(r) (1 - F_\Gamma(x/\beta)). \end{aligned}$$

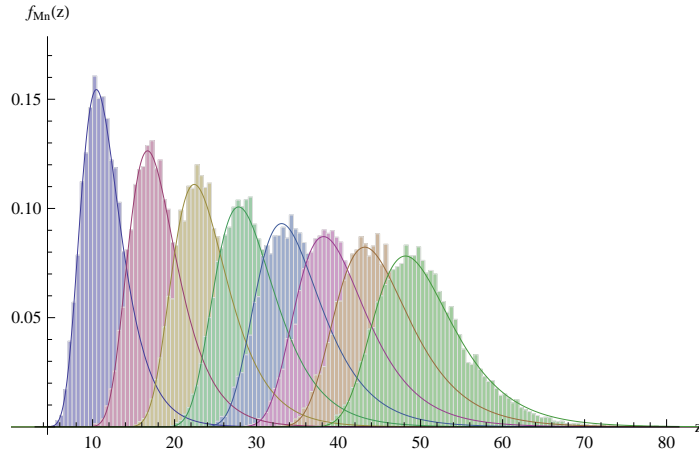


Figure 1: Convergence of the distribution of the maximum to the analytical result. Bars depict the simulation results, while the solid lines depict the analytical results of the max norm distribution with $\{4r\}_{r=1}^8$ degrees of freedom, respectively. The graphs are given for $K = 30$ users.

Accordingly, for $x = b_{\{n,r\}}$ we obtain,

$$\begin{aligned} a_{\{n,r\}} &= h(b_{\{n,r\}}/\beta) \\ &= \frac{\beta}{n} \Gamma(r) \exp \left\{ Q^{-1} \left(r, \frac{1}{n} \right) \right\} Q^{-1} \left(r, \frac{1}{n} \right)^{1-r}. \end{aligned}$$

□

Figures 1 and 2 depict the simulation results versus the analytical results of the EVT with the new normalizing constants derived herein ($a_{\{n,r\}}$ and $b_{\{n,r\}}$ given in (4) and (5), respectively). The maximum of K χ^2 -distributed random variables is compared to the Gumbel distribution predicted by EVT. Figure 1 depicts the case where $K = 30$ while in Figure 2 for $K = 300$. In both cases, figures are plotted for several values of receiving antennas (r). Tight convergence is clearly visible, with reasonable approximation even for 30 users.

To see how the new normalizing constants relate to the previous ones reported in the literature, Figure 3 depicts the value of $a_{\{n,r\}}$ for several values of r , as n increases. While the new constant converges to 2 slowly, it is constant for moderate values of n , hence the tight convergence of *the distribution of the maximum to the Gumbel distribution*.

3.3 Linear Receivers

As we aim at analysing the capacity under practical constraints such as scheduling only a subset of the users in each time slot, we focus our attention on linear decoding at the BS. Such decoders, such as the ZF decoder or the MMSE decoder, are indeed widely used in practice. Hence, the analysis in this paper will be based on either linear decorrelation (Section 4) or the MMSE receiver (Section 6), assuming optimal coding of the resulting single user Gaussian channels, given the effective Signal to Noise Ratio (SNR).

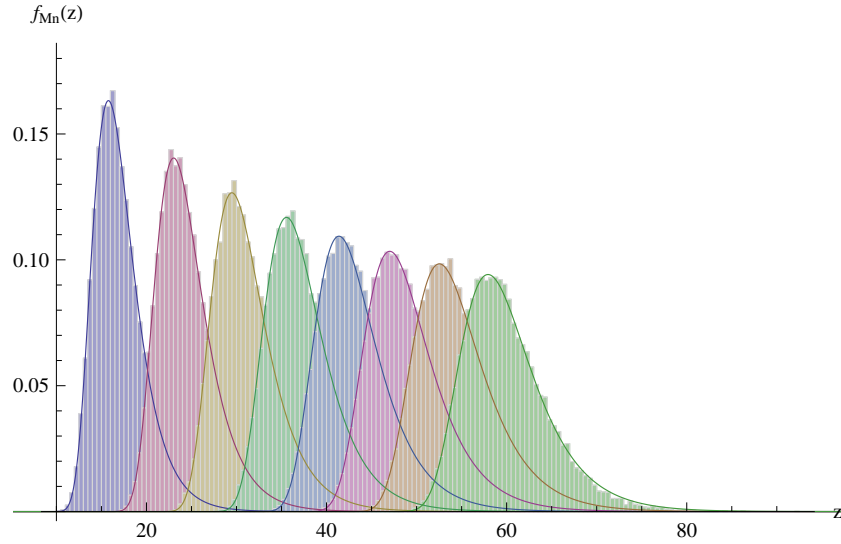


Figure 2: Convergence of the distribution of the maximum to the analytical result. Bars depict the simulation results, while the solid lines depict the analytical results of the max norm distribution with $\{4r\}_{r=1}^8$ degrees of freedom, respectively. The graphs are given for $K = 300$ users.

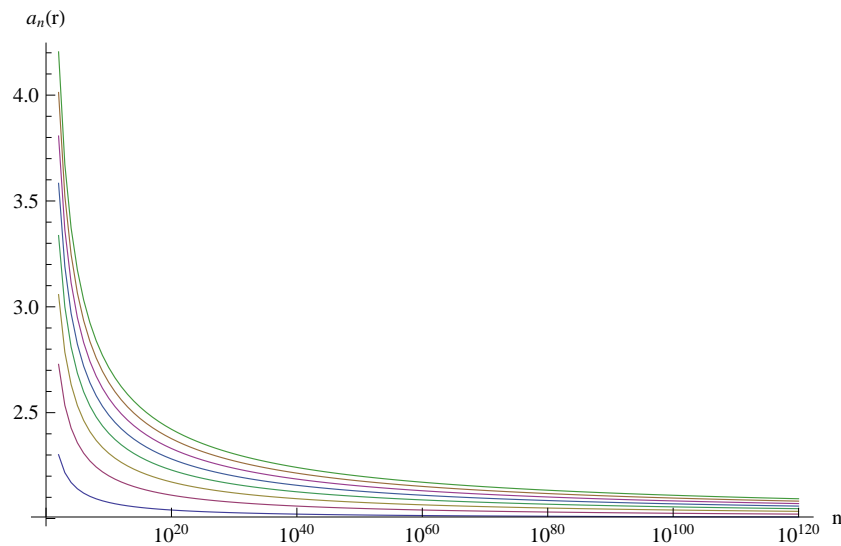


Figure 3: Convergence of the normalizing constant $a_{\{n,r\}}$ for $r = \{2i\}_{i=1}^8$ receiving antennas to the limit $a_n = 2$. Note that this slow convergence does not affect the convergence of the actual distribution, as the values of $a_{\{n,r\}}$ are within a constant factor from 2 even for very moderate n .

Algorithm: Zero-Forcing receiver

Data: $\{\mathbf{h}_j\}_{j=1}^k$

Result: $\{s_j\}_{j=1}^k$

for $j \leftarrow 1$ **to** k **do**

$\tilde{\mathbf{H}} \leftarrow [\mathbf{h}_1 \cdots \mathbf{h}_{j-1} \mathbf{h}_{j+1} \cdots \mathbf{h}_k]$;

$\mathbf{V}_j \leftarrow \text{nullspace}(\tilde{\mathbf{H}})$;

$s_j \leftarrow \mathbf{V}_j \mathbf{y} = \mathbf{V}_j \mathbf{h}_j \mathbf{x}_j + \mathbf{V}_j \mathbf{w}$;

end

Figure 4: Zero Forcing decoder.

Specifically, for the ZF receiver, focusing on the signal received from the j th user, rewrite (1) as:

$$\mathbf{y} = \mathbf{h}_j \mathbf{x}_j + \sum_{i \neq j}^k \mathbf{h}_i \mathbf{x}_i + \mathbf{w}.$$

Let \mathbf{V}_j be a unitary matrix representing the null space of the subspace spanned by $\{\mathbf{h}_i\}_{i \neq j}$. Since the entries of the channel vectors are i.i.d., when k users transmit the subspace spanned by the vectors $\{\mathbf{h}_i\}_{i \neq j}$ has rank $k - 1$ with probability one [40, Chapter 8]. Thus, to decode, the receiver projects the received vector \mathbf{y} on the subspace spanned by \mathbf{V}_j , and nulls the inter-stream interference. Finally, the signal of user j can be demodulated using a matched filter (i.e., maximal ratio combiner). The algorithm is given in Figure 4. Note that a full degrees-of-freedom gain is attained when r users transmit. In this case, $\dim(\mathbf{V}_j) = 1$, and $\|\mathbf{V}_j \mathbf{h}_j\|^2 \sim \chi_2^2$, e.g., [40]. Accordingly, when using a ZF receiver, we aim at algorithms which select at most r users (of the available K) in each time slot. As mentioned, since we focus on the scenario in which $K \gg r$, the set of selected users has a crucial effect on the system capacity. Optimally, a BS would receive CSI from all users, and schedule the r best users for transmission. Under the linear decorrelation above, the resulting expected capacity is

$$\max_{\mathcal{I} \subset \{1, \dots, K\}, |\mathcal{I}|=r} \sum_{i \in \mathcal{I}} E \log(1 + P \|\mathbf{V}_i \mathbf{h}_i\|^2)$$

However, we wish to avoid the overhead and complexity of such a centralized process, and select a group of users, approximating the optimal selection, distributively.

While simple and intuitive, the ZF receiver is limited in its performance. The MMSE receiver, however, although still linear, maximizes the mutual information and hence achieves better performance (e.g. [40, 7, 6]). In this receiver, to decode the i th data stream, the receiver treats the rest of the streams as noise. It then whitens the resulting colored noise and uses a matched filter to obtain maximum SINR.

Let \mathbf{H} be a matrix whose columns are the channel vectors of the transmitting users. Similarly, let $\mathbf{H}_{(-i)}$ be the matrix \mathbf{H} with its i th column removed and define

$$\mathbf{R} = \left(\mathbf{H}_{(-i)} \mathbf{H}_{(-i)}^\dagger + I \right)^{-1}. \quad (6)$$

Then, the corresponding output SINR _{i} on the stream i can be expressed by [6]:

$$\text{SINR}_i = \mathbf{h}_i^\dagger \mathbf{R} \mathbf{h}_i. \quad (7)$$

This SINR value will be at the basis of our analysis in Section 6.

Algorithm: Channel-Access

Data: \mathbf{h}_i, u_k

```
if  $\|\mathbf{h}_i\|^2 > u_k$  then
| transmit
else
| keep silent
end
```

Figure 5: A simple channel access algorithm.

4 A Distributed Algorithm

A common approach to select a single user distributively, is a threshold-based procedure, in which a capacity threshold is set, and only a user who exceeds it transmits ([29, 26]). Of course, the events in which none of the users or several users exceed the threshold should be taken into account. In this paper, however, we wish to select a group of users, and analyze the resulting capacity.

At the heart of the algorithms we suggest herein, stands a similar threshold-based procedure. However, the challenge is twofold. First, in selecting a threshold such that a favorable *group of users* exceed it. Second, in analyzing the results under the various decoding procedures and at the limit of large K . When doing this, a few important questions arise: On which variable should a threshold be set and how many users will pass it? How can one assess the mutual interference between the users which passed? What will be the loss in this distributed procedure compared to the optimal, centralized one?

In the next three sections, we answer the above questions. We set a threshold on the *channel norms*, and analyze the resulting exceedance rate. We further analyze the mutual interference, in terms of the *angles* between the exceeding users, and conclude by analysing the resulting *sum capacity*, showing that a distributed algorithm can achieve the *same scaling laws* as a centralized one.

In particular, we suggest two distributed algorithms. In the first, described in this section, a single threshold is utilized when decoding is done using linear decorrelation. In the second, described in Section 5, we offer a *set of thresholds* to match a Successive Interference Cancellation (SIC) procedure.

Given the number of users K , we set a threshold u_k on the norm $\|\mathbf{h}\|^2$, such that $k \leq r$ strongest users exceed it on average. In each slot, each user estimates its channel's norm. A user with a norm greater than the threshold, transmits. We assume the transmission includes the channel vector as a low-rate preamble so the BS has the CSI *of the transmitting users*. The algorithm for user i is given in Figure 5.

Note that the receiver cannot recover more than r data streams. That is, since for more than r users the performance (both under ZF decoding and MMSE decoding in Section 6) deteriorates significantly, if more than r users begin transmission simultaneously, we assume a collision occurs and the whole slot is lost (zero capacity). Similarly, since users act independently, a slot might be idle, if no user exceeded the threshold. Thus, we say that a slot is utilized if at least one user, but no more than r users, are transmitting.

The first result, Proposition 1 below, gives the sum capacity under the above distributed user selection algorithm and ZF decoding. Note that this simple proposition still includes an

expectation on the channel vectors seen by the users, hence cannot give the understanding we wish regarding the sum capacity under the suggested algorithm. Still, it will be the starting point, from which we will derive the bounds which give the right insight and scaling laws.

Proposition 1. *For $K \gg r$, the expected sum capacity of Algorithm CHANNEL-ACCESS with ZF decoding is given by*

$$EC(u_k) = \sum_{j=1}^r \frac{k^j e^{-k}}{j!} \sum_{i=1}^j E \left[\log \left(1 + P \|\mathbf{V}_i \mathbf{h}_i\|^2 \right) \middle| \|\mathbf{h}_i\|^2 > u_k \right] + O \left(\frac{\log \log K}{K} \right),$$

where k , to be optimized, is the expected number of users to exceed the threshold u_k , the $\{\mathbf{h}_i\}_{i=1}^{j \leq r}$ are the channel vectors of the users who exceeded the threshold and $\{\mathbf{V}_i\}_{i=1}^{j \leq r}$ are the corresponding null spaces.

Proof. According to the law of total probability, we express the expected capacity in a slot by summing over the number of users who exceed the threshold, and the sum capacity these users see, given that they exceeded the threshold. As mentioned, if more than r users are transmitting in a slot, the receiver cannot successfully null the inter-stream interference, and the capacity in that slot is zero.

Hence, the expected capacity has the form:

$$\sum_{j=1}^r \Pr\{j \text{ users exceed}\} \sum_{i=1}^j E [C_i | \|\mathbf{h}_i\|^2 > u_k].$$

When the users are i.i.d., the probability of j threshold exceedances follows the binomial distribution with probability $p = k/K$ to exceed the threshold. Since we consider large K and small values of k , the number of users to exceed threshold can be approximated by the Poisson distribution with an approximation error in the order of $1/K$. This is based on the Poisson Point Process Approximation developed in [29] for the single-user scenario. In short, this method gives a Poisson approximation for the number of users exceeding a high threshold u_k . However, as this approximation error is within the sum, it is multiplied by the individual capacities, which scales like the optimal scaling law of the multi-user diversity when a single, strongest user, is scheduled, i.e., $\Theta(\log \log K)$ (see e.g., [21, 18] and the references therein). Hence, the $O\left(\frac{\log \log K}{K}\right)$ approximation error. Finally, note that the number of exceeding users j affects the effective SNR seen by the attending users. In particular, when j users exceed threshold, the dimension of \mathbf{V}_i is $(r - j + 1) \times r$. Thus, as j decreases, the signal of the attending users is projected on a less restrictive null-space. Accordingly, each stream may spread on more receiving antennas in the ZF process, which leads to a higher power gain (for details on ZF decoding, see [40]). Nonetheless, the reader should not be confused. The highest capacity is attained when r users utilize the channel simultaneously to achieve a full degrees-of-freedom gain. \square

To ease notation, the $O\left(\frac{\log \log K}{K}\right)$ approximation error is omitted from now on.

To evaluate the result in Proposition 1, the behavior of $\|\mathbf{V}_i \mathbf{h}_i\|^2$ should be understood, especially considering the fact that the number of users exceeding the threshold is random. To this end, the following upper and lower bounds are useful. These bounds will be the basis of the scaling laws we derive.

Lemma 1. *The expected sum capacity of Algorithm CHANNEL-ACCESS with ZF decoding satisfies the following upper bound*

$$EC(u_k) \leq \sum_{j=1}^r \frac{k^j e^{-k}}{j!} j \log \left(1 + \frac{P}{r} (r - j + 1) (u_k + a_{\{K,r\}}) \right),$$

where $a_{\{K,r\}}$ is given by (4) and u_k is the threshold set such that k users exceed it on average.

The bound in Lemma 1, while not giving the exact capacity, still depicts the essence of the system behavior. To understand its implications, we note the following: We set a threshold such that k out of the K users exceed it on average. I.e., the average exceedance rate is k . Indeed, the expression $\frac{k^j e^{-k}}{j!}$ in the sum over j gives the probability for exactly j users exceeding. Each of the j users, under zero forcing, experiences a single user channel, with its power P scaled according to two factors: (i) a multiplication by $(u_k + a_{\{K,r\}})$, as this is the average norm of its channel vector, where u_k is the threshold exceeded, and a_K is the average distance *above* the threshold. (ii) a multiplication by $\frac{r-j+1}{r}$, as in case only $j < r$ users exceeded the threshold, the zero forcing algorithm does not have to cancel $r - 1$ users, only $j - 1$, hence the null space has a larger dimension, yet the number of receive antennas is r . As the threshold u_K will be shown to be $\Theta(\log K)$, the optimal scaling law will follow. A complete discussion will be given after the lower bound is introduced. Indeed, as it turns out in the simulation results, the bound in Lemma 1 is tight even for relatively small number of antennas and users. Note, however, that if less than r users exceed, as a higher SNR can be attained at the receiver, in order to achieve the capacity in this case, a user must know how many users exceeded, so it can exploit the high SNR for, e.g., higher transmission rate. Hence, we require that the number of users that actually exceeded the threshold will be announced.

Remark 2. *Note that in practice it is beneficial to choose k slightly smaller than the number of antennas r . This is since if less than r users exceed, the SNR seen by each user is only larger, yet if more than r users exceed, the slot is lost.*

Proof (Lemma 1). We start with Proposition 1. By Jensen inequality,

$$\begin{aligned} EC(u_k) &= \sum_{j=1}^r \frac{k^j e^{-k}}{j!} \sum_{i=1}^j \mathbb{E} \left[\log \left(1 + P \|\mathbf{V}_i \mathbf{h}_i\|^2 \right) \middle| \|\mathbf{h}_i\|^2 > u_k \right] \\ &\leq \sum_{j=1}^r \frac{k^j e^{-k}}{j!} \sum_{i=1}^j \log \left(1 + P \mathbb{E} \left[\|\mathbf{V}_i \mathbf{h}_i\|^2 \middle| \|\mathbf{h}_i\|^2 > u_k \right] \right). \end{aligned} \quad (8)$$

Consider the norm $\|\mathbf{V}_i \mathbf{h}_i\|^2$, where \mathbf{V}_i has $r - j + 1$ rows. Denoting by $\mathbf{V}_i^{(m)}$ the m th row of

\mathbf{V}_i , we have

$$\begin{aligned}
\mathbb{E}[\|\mathbf{V}_i \mathbf{h}_i\|^2 \mid \|\mathbf{h}_i\|^2 > u_k] &= \mathbb{E} \left[\sum_{m=1}^{r-j+1} |\langle \mathbf{V}_i^{(m)}, \mathbf{h}_i \rangle|^2 \mid \|\mathbf{h}_i\|^2 > u_k \right] \\
&\stackrel{(a)}{=} \sum_{m=1}^{r-j+1} \mathbb{E} \left[\|\mathbf{h}_i\|^2 \frac{|\langle \mathbf{V}_i^{(m)}, \mathbf{h}_i \rangle|^2}{\|\mathbf{h}_i\|^2 \|\mathbf{V}_i^{(m)}\|^2} \mid \|\mathbf{h}_i\|^2 > u_k \right] \\
&\stackrel{(b)}{=} \mathbb{E}[\|\mathbf{h}_i\|^2 \mid \|\mathbf{h}_i\|^2 > u_k] \sum_{m=1}^{r-j+1} \mathbb{E} \left[\frac{|\langle \mathbf{V}_i^{(m)}, \mathbf{h}_i \rangle|^2}{\|\mathbf{h}_i\|^2 \|\mathbf{V}_i^{(m)}\|^2} \right] \\
&\stackrel{(c)}{=} \mathbb{E}[\|\mathbf{h}_i\|^2 \mid \|\mathbf{h}_i\|^2 > u_k] (r-j+1) \int_0^1 (1-\alpha)^{r-1} d\alpha \\
&\stackrel{(d)}{=} (u_k + a_K)(r-j+1) \frac{1}{r}.
\end{aligned}$$

In the above chain of equalities, (a) is since $\|\mathbf{V}_i^{(m)}\|^2 = 1$ (b) is since \mathbf{h}_i is a random i.i.d. complex normal vector, and the squared-normalized inner product $\frac{|\langle \mathbf{V}_i^{(m)}, \mathbf{h}_i \rangle|^2}{\|\mathbf{h}_i\|^2 \|\mathbf{V}_i^{(m)}\|^2}$ is its angle from $\mathbf{V}_i^{(m)}$, a vector in the null space of $\{\mathbf{h}_l\}_{l \neq i}$. Since these vectors are independent of \mathbf{h}_i , this angle is independent of the norm of \mathbf{h}_i (c) is since the distributions of the norms and angles are independent of m , and since, by [24, Lemma 3.2], the angle has the same distribution as the minimum of $r-1$ independent uniform $[0, 1]$ random variables (i.e., with CDF $1 - (1-\alpha)^{r-1}$, $0 \leq \alpha \leq 1$) (d) is the result of computing the expected norm of an i.i.d. complex normal random vector, *given that it is above a threshold which is exceeded by only k out of K norms on average*. The details are in Corollary 1, Section 7.

Substituting in (8), we have

$$\begin{aligned}
EC(u_k) &\leq \sum_{j=1}^r \frac{k^j e^{-k}}{j!} \sum_{i=1}^j \log \left(1 + \frac{P}{r} (u_k + a_{\{K,r\}})(r-j+1) \right) \\
&\leq \sum_{j=1}^r \frac{k^j e^{-k}}{j!} j \log \left(1 + \frac{P}{r} (u_k + a_K)(r-j+1) \right),
\end{aligned}$$

which completes the proof. \square

We now present a corresponding lower bound.

Lemma 2. *The expected sum capacity of Algorithm CHANNEL-ACCESS with ZF decoding satisfies the following lower bound.*

$$EC(u_k) \geq \left(\sum_{j=1}^r \frac{k^j e^{-k}}{j!} j \right) (r-1) \int_0^1 (1-\alpha)^{r-2} \log(1 + Pu_k \alpha) d\alpha,$$

where u_k is a threshold set such that k users exceed it on average.

It is important to note that the integral in Lemma 2 above has a finite series expansion with r summands. This finite series has $\log(1 + Pu_k)$ at the leading term, resulting in the expected scaling law. We describe it in Claim 2 below, within the proof of the main result in this section - Theorem 2.

Proof. Following the derivations of the upper bound, we have

$$\begin{aligned}
EC(u_k) &= \sum_{j=1}^r \frac{k^j e^{-k}}{j!} \sum_{i=1}^j \mathbb{E} \left[\log \left(1 + P \sum_{m=1}^{r-j+1} \|\mathbf{h}_i\|^2 \frac{\langle \mathbf{V}_i^{(m)}, \mathbf{h}_i \rangle^2}{\|\mathbf{h}_i\|^2 \|\mathbf{V}_i^{(m)}\|^2} \right) \middle| \|\mathbf{h}_i\|^2 > u_k \right] \\
&\stackrel{(a)}{\geq} \sum_{j=1}^r \frac{k^j e^{-k}}{j!} \sum_{i=1}^j \mathbb{E} \log \left(1 + Pu_k \sum_{m=1}^{r-j+1} \frac{\langle \mathbf{V}_i^{(m)}, \mathbf{h}_i \rangle^2}{\|\mathbf{h}_i\|^2 \|\mathbf{V}_i^{(m)}\|^2} \right) \\
&\stackrel{(b)}{=} \sum_{j=1}^r \frac{k^j e^{-k}}{j!} j \mathbb{E} \log \left(1 + Pu_k \sum_{m=1}^{r-j+1} \frac{\langle \mathbf{V}_{i'}^{(m)}, \mathbf{h}_{i'} \rangle^2}{\|\mathbf{h}_{i'}\|^2 \|\mathbf{V}_{i'}^{(m)}\|^2} \right) \\
&\geq \sum_{j=1}^r \frac{k^j e^{-k}}{j!} j \mathbb{E} \log \left(1 + Pu_k \frac{\langle \mathbf{V}_{i'}^{(1)}, \mathbf{h}_{i'} \rangle^2}{\|\mathbf{h}_{i'}\|^2 \|\mathbf{V}_{i'}^{(1)}\|^2} \right) \\
&\stackrel{(c)}{=} \sum_{j=1}^r \frac{k^j e^{-k}}{j!} j \int_0^1 (r-1)(1-\alpha)^{r-2} \log(1 + Pu_k \alpha) d\alpha
\end{aligned}$$

where (a) is since the norms of *all users participating* are above the threshold u_k ; (b) is since the angles in the inner sum are identically distributed and independent of i , hence an arbitrary $1 \leq i' \leq j$ can be used; (c) is by explicitly computing the expectation over the angle between \mathbf{h}_i and $\mathbf{V}_i^{(1)}$, remembering that it has a density $(r-1)(1-\alpha)^{r-2}$ for $0 \leq \alpha \leq 1$. This completes the proof. \square

The results above lead to the following scaling law, which is the main result in this section. It asserts that the scaling law of $r \log(P \log K)$ for the sum rate in a multi-user system can in fact *be achieved distributively*, without collecting all channel states from all users and scheduling them in a centralized manner. In other words, the threshold based algorithm suggested selects an optimal *set of users* (asymptotically in the number of users) distributively and without any cooperation. This is summarized in the next theorem.

Theorem 2. *The expected sum capacity of Algorithm CHANNEL-ACCESS with ZF decoding scales as $\Theta(r \log(P \log K))$ for large enough number of users K .*

Proof. By Lemma 1,

$$\begin{aligned}
EC(u_k) &\leq \sum_{j=1}^r \frac{k^j e^{-k}}{j!} j \log \left(1 + P \frac{(r-j+1)(u_k + a_K)}{r} \right) \\
&\leq \sum_{j=1}^r \frac{k^j e^{-k}}{j!} j \log \left(1 + P(u_k + a_K) \right) \\
&\leq r \log \left(1 + P(u_k + a_K) \right).
\end{aligned}$$

On the other hand, consider the lower bound given in Lemma 2. Since k is a parameter to be optimized, the optimum is at least as large as when choosing $k = r$. We have

$$\sum_{j=1}^r \frac{r^j e^{-r}}{j!} j = r \sum_{j=0}^{r-1} \frac{r^j e^{-r}}{j!} j \geq 0.4r,$$

where the last inequality is by evaluating the sum at $r = 2$. Note that larger values of r give only slightly larger values, with a limit of 0.5 as $r \rightarrow \infty$.¹

Now, consider the integral over α in Lemma 2. In Section 7, we prove the following claim.

Claim 2. *The integral over α in Lemma 2 has the following finite series expansion:*

$$\begin{aligned} (r-1) \int_0^1 (1-\alpha)^{r-2} \log(1+Pu\alpha) d\alpha \\ = \left(\frac{1+Pu}{Pu}\right)^{r-1} \log(1+Pu) - \sum_{i=0}^{r-2} \left(\frac{1+Pu}{Pu}\right)^i \frac{1}{r-1-i}. \end{aligned}$$

This gives a finite series expansion for the integral, in terms of the power P and the threshold u . For example, for $r = 4$ we have

$$\begin{aligned} (r-1) \int_0^1 (1-\alpha)^{r-2} \log(1+Pu\alpha) d\alpha \\ = \frac{6(1+Pu)^3 \log(1+Pu) - 2u^3 P^3 - 3u^2 P^2(1+Pu) - 6uP(1+Pu)^2}{6u^3 p^3}. \quad (9) \end{aligned}$$

Thus, the integral can be easily approximated by $\log(1+Pu) + O\left(\frac{\log u}{u}\right)$.

Since we consider the regime of large enough number of users K , yet a finite number of antennas r , we have $k = O(1)$ and as a result $u_k = \Theta(\log K)$. In fact, since the distribution of the projected channel gain seen by a user in this decoding scheme is the exponential distribution with rate $1/2$, it can be shown that $u_k = 2(\log K - \log k)$ (we discuss the threshold value in detail in Section 7.2). This gives rise to the $\Theta(r \log(P \log K))$ scaling law. \square

Remark 3. *It is well known that linear decorrelation is asymptotically optimal at high SNR. The suggested algorithms pick the users with the highest SNR, accordingly, they operate at high SNR and loose only a constant fraction of the optimal centralized scheduling scheme.*

Extensive simulations were conducted to compare the analytical bounds derived above to real world situations with a finite number of users. In Figure 6, we compare the bounds on the expected capacity of the threshold-based scheduling scheme under ZF-receiver (i.e., Lemma 1 and Lemma 2), to the simulation results. The bounds and simulation are for $K = 300$ users, with 2, 4 and 8 receiving antennas at the BS. The tightness of the upper bound is clearly visible. While the lower bound is looser, it still gives the correct behaviour as a function of the number of users passing the threshold on average, k . Indeed, it is clear from the figure that a key factor affecting the system performance is the number of users passing the threshold. This distribution gives the graphs their Poisson-like shape.

To see that the trend holds even for a relatively small number of users, Figure 7 includes the same plots for $K = 30$. Note that even for 30 users the algorithm manages to achieve a significant rate (compared, e.g., to the one achieved with 300 users). This means the essence of the multi-user diversity is exploited by the algorithm even for a relatively small number of users. Note, however, that as r approaches K then the accuracy of the bounds decreases.

¹This is the CDF of a Poisson random variable with parameter r , calculated at $r - 1$. The limiting behavior can be found in [41].

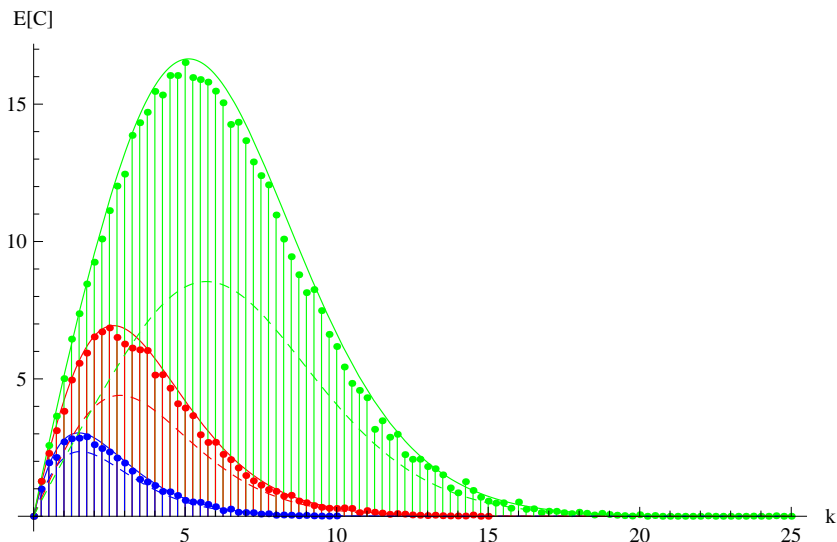


Figure 6: Expected capacity under a single threshold algorithm and $K = 300$. Bars are simulation results, while the solid and dashed lines represent the upper and lower bounds, respectively. The threshold u_k is set such that k users exceed it on average. The green (upper), red (middle) and blue (lower) lobes are for $r = 8, 4$ and 2 receive antennas, respectively. Note that the optimal k is smaller than r . This is since it is better to aim at slightly less than r users passing, as the performance deteriorates significantly for more than r users transmitting concurrently.

The results in Figure 6 and Figure 7 give the expected sum capacity as a function of k . The capacity distribution, compared to different algorithms, will be given in the subsequent sections.

5 A Multi-Threshold, SIC-Based Algorithm

In the previous section, only a single threshold was used, and a user’s data was decoded by projecting the received signal on the null space of the sub-space spanned by the channels of the interfering users. While this algorithm managed to capture the key performance-enhancing aspects of the multi-user system, and achieve the optimal scaling laws distributively, better results can be expected for low to moderate number of users. In that regime, harnessing additional multiple access techniques and a more sophisticated thresholding algorithm can achieve better performance. In this section, we see that this is indeed so.

When using SIC [40, Ch.6], the decoder uses the decoded signal of a previous user to decode the next one (by subtracting it from the received stream). After $r - 1$ iterations of SIC, all data streams are decoded. With this in mind, we derive a second, iterative algorithm, to further utilizing the benefits of SIC in a threshold based algorithm. At first glance, for large number of users, a *set of thresholds* $\{u^{(l)}\}$ should be chosen, such that in each iteration only a single user exceeds on average. This way, one can adapt the thresholds set according to the users “admitted” thus far (that is, users who already passed). For example, one can set the next threshold based on the angles of the previously admitted users.

However, it is very likely that in some of the r iterations, more than one user, or no user,

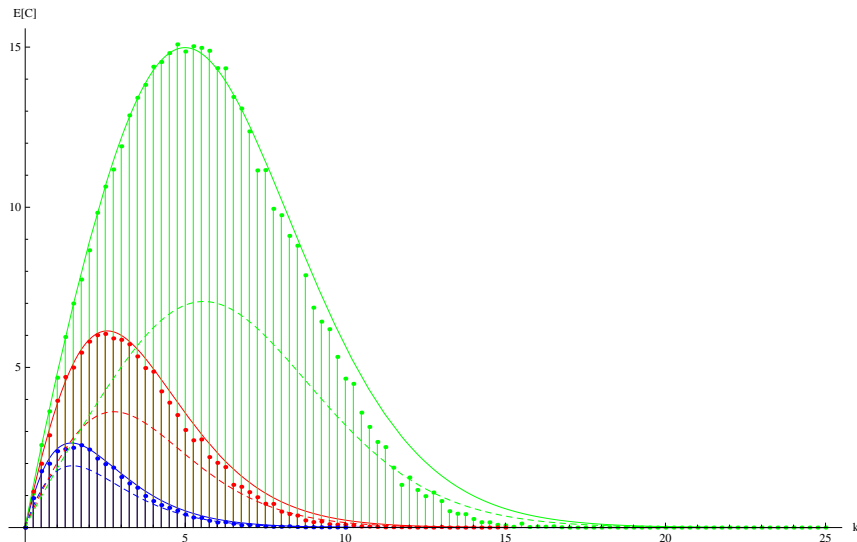


Figure 7: Expected capacity under a single threshold algorithm and $K = 30$. Bars are simulation results, while the solid and dashed lines represent the upper and lower bounds, respectively. The threshold u_k is set such that k users exceed it on average. The green (upper), red (middle) and blue (lower) lobes are for $r = 8, 4$ and 2 receive antennas, respectively. Note that the essence of the analysis holds for even a relatively small number of users as 30 , as the bounds still depict the key elements affecting the performance.

will exceed the threshold. Specifically, the probability that exactly one user will exceed in an iteration is approximately $1/e$. Yet, if a carrier sense, or collision detection mechanism is available, collisions can be resolved by allocating a few mini-slots devoted to finding the strongest user in each iteration [26, 29].

This gives rise to the following algorithm: After the strongest user is found, it begins its transmission by announcing its channel vector. In the l th iteration, the rest of the users project their channel vector on the orthonormal basis $\mathbf{V}^{(l-1)}$, which spans the null space of the channels vectors announced thus far. Now, the scheduled user for iteration l is the one with the *strongest projection*. The process ends when r users are selected. Note that this involves announcements of the channel vectors only from the $r \ll K$ selected users. The algorithm is described in Figure 8.

When a user projects its channel on $\mathbf{V}^{(l-1)}$, the resulting gain distribution follows the χ^2 -distribution with $2(r-l+1)$ degrees of freedom [40]. That is, $\|\mathbf{V}^{(l-1)}\mathbf{h}\|^2 \sim \chi_{2(r-l+1)}^2$. Let $\mathbf{h}^{(l)}$ be the channel with the strongest norm in iteration l , i.e.,

$$\mathbf{h}^{(l)} = \max_{1 \leq i \leq K} \|\mathbf{V}^{(l-1)}\mathbf{h}_i\|^2.$$

Note that in practice, the BS *does not have to search for the maximum above*, but, instead, a threshold is set, only the strongest users pass, and one is selected using a collision resolution mechanism. Utilizing the EVT for the $\chi_{2(r-l+1)}^2$ -distribution, the norm $\|\mathbf{h}^{(l)}\|^2$ can then be characterized. We have the following.

Proposition 2. *For sufficiently large K , the expected sum capacity of Algorithm SIC-*

Algorithm: SIC-Channel-Access**Data:** Channel vector \mathbf{h} $\tilde{H} \leftarrow \{\}; \mathbf{V}^{(0)} \leftarrow I_{r \times r};$ **for** $l \leftarrow 1$ **to** r **do** $u^{(l)} \leftarrow Q^{-1}(r - l + 1, \frac{1}{K});$ $\mathbf{h}_o \leftarrow \mathbf{V}^{(l-1)}\mathbf{h};$ **if** $\|\mathbf{h}_o\|^2 > u^{(l)}$ **then** | transmit \mathbf{h} **else** | receive \mathbf{h}' ; $\tilde{H} \leftarrow \tilde{H} \cup \mathbf{h}'$; $\mathbf{V}^{(l)} \leftarrow \text{nullspace}(\tilde{H});$ **end****end**

Figure 8: A multi-threshold, SIC-based channel access algorithm.

CHANNEL-ACCESS with ZF-SIC decoding is given by:

$$C_{av}(\{u^{(l)}\}_{l=1}^r) = \sum_{l=1}^r E[\log(1 + P\|\mathbf{h}^{(l)}\|^2)],$$

where $\mathbf{h}^{(l)}$ is the channel vector of with the largest norm after the l_{th} projection.

Note that the above result assumes each transmitting user can adapt its transmission rate to be decoded successfully at the base station. This is possible as each user *knows the channel vectors on the interfering users* and his own channel vector, thus can calculate the SNR the BS will experience when decoding. Furthermore, a splitting algorithm is used [26], hence the Poisson coefficients can be omitted.

Again, to evaluate the performance of Proposition 2, the distribution of $\|\mathbf{h}^{(l)}\|^2$ should be examined. We now derive upper and lower bounds to better evaluate the performance under the suggested algorithm.

Lemma 3. *The expected sum capacity of Algorithm SIC-CHANNEL-ACCESS with ZF-SIC decoding satisfies the following upper bound.*

$$C_{av} \leq \sum_{l=1}^r \log(1 + P(b_{\{K,r-l+1\}} + \gamma a_{\{K,r-l+1\}})),$$

where $a_{\{K,r-l+1\}}, b_{\{K,r-l+1\}}$ are the normalizing constant given in (4) and (5) respectively, and $\gamma \approx 0.57$ is the Euler Gamma constant.

Note that $b_{\{K,r-l+1\}} = \Theta(\log K)$ (as it converges to b_K in equation (3)), hence the same scaling law is achieved.

Proof. By Jensen inequality,

$$\begin{aligned}
C_{av}(\{u^{(l)}\}_{l=1}^r) &= \sum_{l=1}^r \mathbb{E} \left[\log \left(1 + P \|\mathbf{h}^{(l)}\|^2 \right) \right] \\
&\leq \sum_{l=1}^r \log \left(1 + P \mathbb{E} \left[\|\mathbf{h}^{(l)}\|^2 \right] \right) \\
&= \sum_{l=1}^r \log \left(1 + P \mathbb{E} \left[\max_{1 \leq i \leq K} \|\mathbf{V}^{(l-1)} \mathbf{h}_i\|^2 \right] \right).
\end{aligned}$$

To analyse the expectation some care is needed. Without conditioning in the l -th iteration on the event that the remaining users did not come out ahead in the previous iterations, that is, “allowing” all users to compete again, the norm $\|\mathbf{V}^{(l-1)} \mathbf{h}_i\|^2$ follows $\chi_{2(r-i+1)}^2$ -distribution. Hence, by Theorem 1, $\max_i \|\mathbf{V}^{(l-1)} \mathbf{h}_i\|^2$ follows the Gumbel distribution, with normalizing constants $a_{\{K, r-l+1\}}$ and $b_{\{K, r-l+1\}}$ given (4) and (5), respectively. However, when such a conditioning is applied, the expectation can only decrease, as the previous users are not allowed to participate. Thus, the expected maximal norm is upper bounded by the expected value of the Gumbel distribution with the above parameters. Lemma 3 then follows. \square

To bound the performance from below, we only derive probabilistic lower bound. That is, a set of fixed relatively low threshold values are computed, such that in each iteration, we can guarantee that the norm of the strongest channel is greater than that value with high probability. However, in order to attain a non-trivial bound, these values need to be as high as possible, yet, maintain the lower bound with high probability. Specifically, in each iteration, we chose a threshold value that is greater than the strongest norm with probability $O(1/K)$ (hence the probability that no user exceeds it is $O(1/K)$). This corresponds to a threshold that $\log K$ users exceed it on average. Nonetheless, depending on the strictness of the bound, a different threshold sets can be chosen. Accordingly, we have the following.

Lemma 4. *The expected sum capacity of Algorithm SIC-CHANNEL-ACCESS with ZF-SIC decoding satisfies the following lower bound with high probability.*

$$C_{av} \geq \sum_{l=1}^r \log(1 + u_{\log K}^{(l)})$$

where $u_{\log K}^{(l)}$ is a threshold such that $\log K$ projected channel norms exceeds it on average, in iteration l .

Proof. Let us consider the probability that the no user exceeds the threshold $u_{\log K}^{(l)}$ on iteration l . This can be expressed as

$$\begin{aligned}
\Pr \left(\|\mathbf{h}^{(l)}\|^2 < u_{\log K}^{(l)} \right) &= \left(1 - \frac{\log K}{K} \right)^K \\
&= O(1/K).
\end{aligned}$$

Since $\log(1+x)$ is monotone,

$$\Pr \left(\log \left(1 + P \|\mathbf{h}^{(l)}\|^2 \right) < \log \left(1 + P u_{\log K}^{(l)} \right) \right) = O(1/K).$$

Let $A^{(l)} = \{\mathbf{h}^{(l)} : \|\mathbf{h}^{(l)}\|^2 > u_{\log K}^{(l)}\}$, namely, the event in which the strongest channel in iteration l is greater than threshold $u_{\log K}^{(l)}$. We have

$$\begin{aligned} \Pr\left(\bigcap_{l=1}^r A^{(l)}\right) &= \overline{\Pr\left(\bigcup_{l=1}^r \overline{A^{(l)}}\right)} \\ &\geq 1 - \sum_{l=1}^r \Pr\left(\overline{A^{(l)}}\right) \\ &= 1 - rO(1/K). \end{aligned}$$

That is, the probability that at least one user exceeds the threshold in each iteration, is greater than $1 - O(1/K)$. As a result, since each l.h.s. element is greater than threshold with high probability, we conclude that

$$\sum_{l=1}^r \log\left(1 + P\|\mathbf{h}^{(l)}\|^2\right) \geq \sum_{l=1}^r \log(1 + u_{\log K}^{(l)}),$$

with high probability. Consequently,

$$\sum_{l=1}^r \mathbb{E}\left[\log\left(1 + P\|\mathbf{h}^{(l)}\|^2\right)\right] \geq \sum_{l=1}^r \log(1 + u_{\log K}^{(l)}).$$

□

Note that the SIC scheme above achieves the same scaling law as the former linear decorrelation scheme (clearly, one cannot do better asymptotically), yet, it also achieves higher power gain, i.e., there is a boost in performance since the effective SNR is increasing in each iteration. This is clearly seen in the simulations below, where the results are clearly better for the finite population we tested. Specifically, Figure 9 depicts the gain of multi-user scheduling with and without SIC, and compares it to scheduling schemes which schedule a single user at a time.

Remark 4. *Note that the capacity distribution in each iteration under SIC can be approximated by the Gumbel distribution. Further, the sum-capacity distribution under SIC is also approximated by the Gumbel distribution, since the Gumbel distribution is infinitely divisible [5]. This is also consistent with Figure 10, which zooms in on the comparison between the capacity distributions: when the receiver uses ZF versus ZF-SIC to decode the data streams.*

Remark 5. *Note that in the suggested SIC algorithm, the users are naturally ordered from the strongest to the l -strongest user. Hence, to improve the sum capacity, one might devise a distributed water-filling algorithm (e.g. [9]), such that each user will invest a power amount proportional to its order.*

6 MMSE receiver

The ZF receiver discussed thus far is on the one hand simple enough to facilitate rigorous analysis, yet, as shown in the previous sections, powerful enough in the sense that with

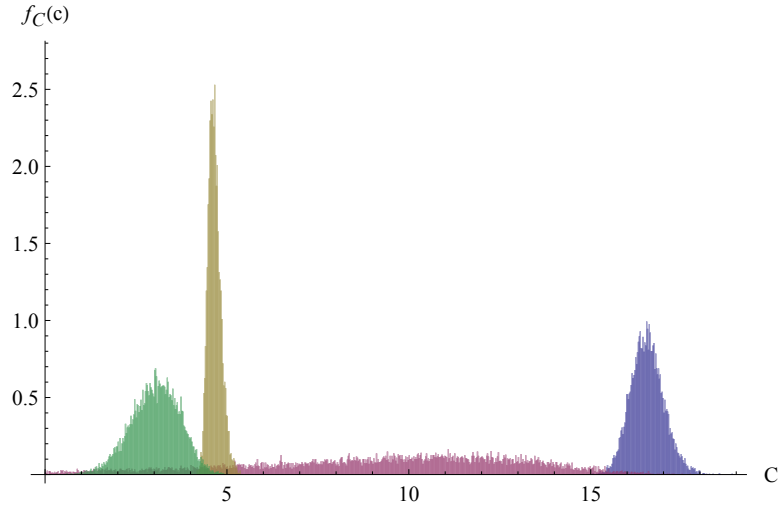


Figure 9: Simulated probability density function of the sum capacity, with $r = 4$ receiving antennas and $K = 300$ users, each with a single transmitting antenna. Green (left): a single arbitrary user is scheduled (approximately Gaussian). Yellow (second left): the strongest user is scheduled (approximately Gumbel). Pink (second right): a group of 4 strongest users are scheduled, with ZF receiver. Blue (right): a group of 4 users are scheduled, with the suggested multi-threshold algorithm and ZF-SIC receiver.

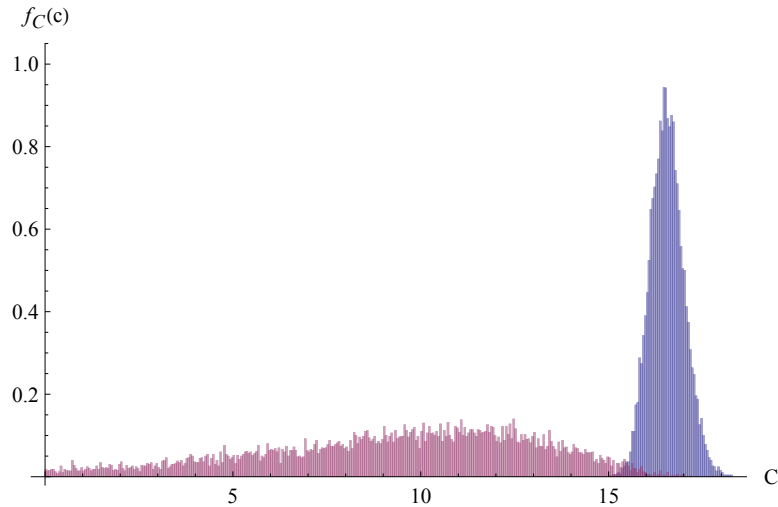


Figure 10: Simulated probability density function of the sum capacity, with $r = 4$ receiving antennas and $K = 300$ users, each with a single transmitting antenna. The left (pink) lobe depicts the capacity when a group of $r = 4$ users are scheduled, and the receiver demodulates the data streams by null forcing (all users are above a threshold, according to the algorithm in Section 4). The right (blue) lobe depicts the capacity when a group of $r = 4$ users are scheduled (using the multi-threshold algorithm), and the receiver demodulates the data streams using SIC.

intelligent user selection (in this paper, distributed) can achieve the optimal scaling laws. Still, this is not the optimal linear receiver. In this section, we explore the scaling laws of the expected capacity of the MMSE receiver.

As mentioned, in this case we let \mathbf{H} denote a matrix whose columns are the channel vectors of the *transmitting users*. That is, when using the CHANNEL-ACCESS algorithm, vectors with norm greater than the threshold. $\mathbf{H}_{(-i)}$ is the matrix \mathbf{H} with its i_{th} column removed. Under these definitions, the SINR seen at the i_{th} stream was given in (7). Let \mathcal{S} denote the set of channels with norm greater than a threshold. Then, the expected capacity under the threshold based scheduling algorithm in Section 4 is as follows.

Proposition 3. *For $K \gg r$, the expected sum capacity with MMSE decoding is*

$$E[C(u_k)] = \sum_{j=1}^r \frac{k^j e^{-k}}{j!} \sum_{i=1}^j E \left[\log \left(1 + P \mathbf{h}_i^\dagger \mathbf{R} \mathbf{h}_i \right) \middle| \|\mathbf{h}_s\|^2 > u_k, \forall s \in \mathcal{S} \right] + O \left(\frac{\log \log K}{K} \right)$$

where u_k is the threshold set such that k users exceed it on average.

This expected capacity should be optimized over k . The proof is similar to the ZF setting. The only change is in the SNR seen by the users, as reflected by the term within the log.

Remark 6. *When ZF decoding was used, the effective SNR seen by a user was $P \|\mathbf{V}_i \mathbf{h}_i\|^2$. As the matrix \mathbf{V}_i is unitary, it is clear why scaling up \mathbf{h}_i resulted in scaling up the SNR. In the MMSE case, however, the analysis is intricate. The SNR is $P \mathbf{h}_i^\dagger \mathbf{R} \mathbf{h}_i$. While \mathbf{h}_i scales up, $\mathbf{R} = (\mathbf{H}_{(-i)} \mathbf{H}_{(-i)}^\dagger + I)^{-1}$ may appear to scale down as the eigenvalues of $\mathbf{H}_{(-i)} \mathbf{H}_{(-i)}^\dagger$ scale up. However, note that $\mathbf{H}_{(-i)} \mathbf{H}_{(-i)}^\dagger$ is not full rank, hence has at least one zero eigenvalue. As a result, \mathbf{R} has at least one eigenvalue which does not scale down.*

To evaluate the expected capacity in Propositions 3, the characteristics of the random variables $\mathbf{h}_i^\dagger \mathbf{R} \mathbf{h}_i$ should be understood, especially when the number of transmitting users is random. Further, the influence of the norms $\|\mathbf{h}_s\|^2$ on $\mathbf{h}_i^\dagger \mathbf{R} \mathbf{h}_i$ should be evaluated. The key technical challenge, however, is due to the norm condition *inducing dependence on the matrix elements*, hence the random matrix theory usually used in the MIMO literature does not hold. Part of the contribution in this section, is by bringing new tools to tackle this problem.

Note that in this section, regular type letters represent random variables as well as scalar variables. The difference will be clear from the context. As a first tool to handle the dependence within the matrix entries, we start with the following claim:

Claim 3. *Assume the norms $\|\mathbf{h}_s\|^2, \forall s \in \mathcal{S}$ are above a given threshold u_k . Then the following properties hold:*

(i) *The entries of the channel vector remain zero mean.*

(ii) *The variance of each entry in the vector scales. In particular, is equals to*

$$E \left[|h_{i,n}|^2 \middle| \|\mathbf{h}_i\|^2 > u_k \right] = (u_k + a_{\{K,r\}}) / r.$$

(iii) *The vector elements remain uncorrelated in pairs.*

Note that, to begin with, the entries of \mathbf{H} are i.i.d. The claim states that conditioned on exceeding a threshold, while not i.i.d., they sustain the zero correlation. This property will be useful throughout the remainder of this paper. The proof of Claim 3 is deferred to Section 7.

6.1 Threshold-based MMSE Upper Bound

Now we are ready to derive the scaling-law of the MMSE receiver, using the following upper and lower bounds on the threshold based expected capacity.

Lemma 5. *The expected sum capacity of Algorithm CHANNEL-ACCESS with MMSE decoding satisfies the following upper bound.*

$$E[C(u_k)] \leq \sum_{j=1}^r \frac{k^j e^{-k}}{j!} j \log \left(1 + P \left(1 - \frac{(j-1)u_k^2}{r \left(\left(1 + \frac{j}{r}\right)(u_k + a_{\{K,r\}}\right)^2 + a_{\{K,r\}}(a_{\{K,r\}} + 1) + u_k \right)} \right) (u_k + a_{\{K,r\}}) \right).$$

where $a_{\{K,r\}}$ is given by (4) and u_k is the threshold set such that k users exceed it on average.

Before we prove the lemma, it is interesting to compare the scaling law under MMSE decoding to that achieved with ZF decoding. In both Lemma 1 and Lemma 5, the capacity seen by each user is approximately $\log(1 + cPu_k)$, for some constant c . Asymptotically, it follows that $0 < c < 1$, and in both cases, the capacity gain comes from the threshold value u_k , which is, as mentioned, $O(\log K)$. This gives the growth rate of $\log \log K$ per user. However, note that while $c = \frac{r-j+1}{r}$ in Lemma 1, for large enough u_k the gain in Lemma 5 is asymptotically $c = \frac{r+1}{r+j}$, that is, a larger gain for any $j \geq 1$. This is not surprising, as an MMSE decoder does give a better power gain, but does not improve the already optimal scaling law.

Proof (Lemma 5). The capacity seen by user i is bounded by:

$$\begin{aligned} E[C_i(u_k)] &\stackrel{(a)}{\leq} \log \left(1 + PE \left[\mathbf{h}_i^\dagger \mathbf{R} \mathbf{h}_i \mid \|\mathbf{h}_s\|^2 > u_k, \forall s \in \mathcal{S} \right] \right) \\ &\stackrel{(b)}{=} \log \left(1 + PE \left[\sum_{n=1}^r \sum_{m=1}^r h_{i,m}^* h_{i,n} [\mathbf{R}]_{mn} \mid \|\mathbf{h}_s\|^2 > u_k, \forall s \in \mathcal{S} \right] \right) \\ &\stackrel{(c)}{=} \log \left(1 + P \sum_{n=1}^r \sum_{m=1}^r E \left[h_{i,m}^* h_{i,n} \mid \|\mathbf{h}_i\|^2 > u_k \right] E \left[[\mathbf{R}]_{mn} \mid \|\mathbf{h}_s\|^2 > u_k, \forall s \in \mathcal{S} \right] \right) \\ &\stackrel{(d)}{=} \log \left(1 + P \sum_{n=1}^r E \left[\|h_{i,n}\|^2 \mid \|\mathbf{h}_i\|^2 > u_k \right] E \left[[\mathbf{R}]_{nn} \mid \|\mathbf{h}_s\|^2 > u_k, \forall s \in \mathcal{S} \right] \right) \\ &\stackrel{(e)}{=} \log \left(1 + P \frac{(u_k + a_{\{K,r\}})}{r} E \left[\text{tr}(\mathbf{R}) \mid \|\mathbf{h}_s\|^2 > u_k, \forall s \in \mathcal{S} \right] \right) \end{aligned} \quad (10)$$

In the above chain of equalities, (a) follows from Jensen inequality. (b) is the equivalent quadric form of $\mathbf{h}_i^\dagger \mathbf{R} \mathbf{h}_i$. (c) is since the vector \mathbf{h}_i is independent in the column vectors of the matrix \mathbf{R} . (d) is since by Claim 3 part (iii), the elements of the vector \mathbf{h}_i are uncorrelated. (e) follows from Claim 3 part (ii).

Now, to address $\text{tr}(\mathbf{R})$, conditioned on $\|\mathbf{h}_s\|^2 > u_k, \forall s \in \mathcal{S}$, we first use the following upper bound on the trace of the inverse of a matrix. For a symmetric $r \times r$ positive definite matrix A [4],

$$\text{tr}(A^{-1}) \leq (\text{tr}(A) \quad r) \begin{pmatrix} \text{tr}(A^\dagger A) & \text{tr}(A) \\ \lambda_{\min}^2(A) & \lambda_{\min}(A) \end{pmatrix}^{-1} \begin{pmatrix} r \\ 1 \end{pmatrix}, \quad (11)$$

where $\lambda_{\min}(A)$ is the smallest eigenvalue of the matrix A . In our case, take $A^{-1} = \mathbf{R}$. To obtain $\lambda_{\min}(\mathbf{R}^{-1})$, we recall that $\mathbf{R}^{-1} = \left(\mathbf{H}_{(-i)} \mathbf{H}_{(-i)}^\dagger + I \right)$ and that $\mathbf{H}_{(-i)} \mathbf{H}_{(-i)}^\dagger$ is an $r \times r$ matrix with rank $j - 1$, with $j \leq r$, thus, by the eigenvalues decomposition theorem, $\mathbf{H}_{(-i)} \mathbf{H}_{(-i)}^\dagger$ has $r - j + 1$ of its eigenvalues equal to zero. Hence, the smallest eigenvalue of \mathbf{R}^{-1} is $\lambda_{\min}(\mathbf{R}^{-1}) = 1$. Thus, using (11), it follows that

$$\begin{aligned} \text{tr}(\mathbf{R}) &\leq \frac{r \left[\text{tr}(\mathbf{R}^{-1}) + \text{tr}(\mathbf{R}^{-\dagger} \mathbf{R}^{-1}) \right] - \text{tr}^2(\mathbf{R}^{-1}) - r^2}{\text{tr}(\mathbf{R}^{-\dagger} \mathbf{R}^{-1}) - \text{tr}(\mathbf{R}^{-1})} \\ &= \frac{r \left[\text{tr} \left(\mathbf{H}_{(-i)} \mathbf{H}_{(-i)}^\dagger \mathbf{H}_{(-i)} \mathbf{H}_{(-i)}^\dagger \right) + \text{tr} \left(\mathbf{H}_{(-i)} \mathbf{H}_{(-i)}^\dagger \right) \right] - \text{tr}^2 \left(\mathbf{H}_{(-i)} \mathbf{H}_{(-i)}^\dagger \right)}{\text{tr} \left(\mathbf{H}_{(-i)} \mathbf{H}_{(-i)}^\dagger \mathbf{H}_{(-i)} \mathbf{H}_{(-i)}^\dagger \right) + \text{tr} \left(\mathbf{H}_{(-i)} \mathbf{H}_{(-i)}^\dagger \right)} \\ &= r - \frac{\text{tr}^2 \left(\mathbf{H}_{(-i)}^\dagger \mathbf{H}_{(-i)} \right)}{\text{tr} \left(\mathbf{H}_{(-i)}^\dagger \mathbf{H}_{(-i)} \mathbf{H}_{(-i)}^\dagger \mathbf{H}_{(-i)} \right) + \text{tr} \left(\mathbf{H}_{(-i)}^\dagger \mathbf{H}_{(-i)} \right)}. \end{aligned}$$

Note that the expression in (10) had a power loss of factor r , that is, P is divided by r . However, it is multiplied by $E \left[\text{tr}(\mathbf{R}) \mid \|\mathbf{h}_s\|^2 > u_k \right]$. In the last equality above we actually see that in this multiplication we gain back a factor of the form $(r - \zeta)$. This suggests that the MMSE decoder is superior to the ZF decoder in terms of power gain, as the expression in the ZF decoder performance does not have this multiplicative factor (this is consistent with, e.g., [40]). We will later evaluate the value of ζ explicitly. Furthermore, note that $\text{tr}(\mathbf{R}^{-\dagger} \mathbf{R}^{-1})$ is actually the squared Frobenius norm of \mathbf{R}^{-1} , which is equal to the sum of squares of its entries. Thus, we have,

$$\begin{aligned} &E \left[\text{tr}(\mathbf{R}) \mid \|\mathbf{h}_s\|^2 > u_k, \forall s \in \mathcal{S} \right] \\ &\leq r - E \left[\frac{\text{tr}^2 \left(\mathbf{H}_{(-i)}^\dagger \mathbf{H}_{(-i)} \right)}{\text{tr} \left(\mathbf{H}_{(-i)}^\dagger \mathbf{H}_{(-i)} \mathbf{H}_{(-i)}^\dagger \mathbf{H}_{(-i)} \right) + \text{tr} \left(\mathbf{H}_{(-i)}^\dagger \mathbf{H}_{(-i)} \right)} \mid \|\mathbf{h}_s\|^2 > u_k, \forall s \in \mathcal{S} \right] \\ &= r - E \left[\frac{\left(\sum_{\substack{n=1 \\ n \neq i}}^j \|\mathbf{h}_n\|^2 \right)^2}{\sum_{\substack{n=1 \\ n \neq i}}^j (\|\mathbf{h}_n\|^2)^2 + 2 \sum_{\substack{n=1 \\ n \neq i}}^j \sum_{\substack{m=n+1 \\ m \neq i}}^j |\langle \mathbf{h}_n, \mathbf{h}_m \rangle|^2 + \sum_{\substack{n=1 \\ n \neq i}}^j \|\mathbf{h}_n\|^2} \mid \|\mathbf{h}_s\|^2 > u_k, \forall s \in \mathcal{S} \right] \\ &= r - E \left[\frac{\left(\sum_{\substack{n=1 \\ n \neq i}}^j \|\mathbf{h}_n\|^2 \right)^2}{\sum_{\substack{n=1 \\ n \neq i}}^j (\|\mathbf{h}_n\|^2)^2 + 2 \sum_{\substack{n=1 \\ n \neq i}}^j \sum_{\substack{m=n+1 \\ m \neq i}}^j \frac{|\langle \mathbf{h}_n, \mathbf{h}_m \rangle|^2}{\|\mathbf{h}_n\|^2 \|\mathbf{h}_m\|^2} \|\mathbf{h}_n\|^2 \|\mathbf{h}_m\|^2 + \sum_{\substack{n=1 \\ n \neq i}}^j \|\mathbf{h}_n\|^2} \mid \|\mathbf{h}_s\|^2 > u_k, \forall s \in \mathcal{S} \right] \end{aligned}$$

where $|\langle \cdot, \cdot \rangle|^2$ is the squared inner product. Note that the numerator inside the expectation

is at least $(j-1)^2 u_k^2$. Thus,

$$\begin{aligned} & \mathbb{E} [\text{tr}(\mathbf{R}) | \|\mathbf{h}_s\|^2 > u_k, \forall s \in \mathcal{S}] \\ & \leq r + \mathbb{E} \left[\frac{-(j-1)^2 u_k^2}{\sum_{\substack{n=1 \\ n \neq i}}^j (\|\mathbf{h}_n\|^2)^2 + 2 \sum_{\substack{n=1 \\ n \neq i}}^j \sum_{\substack{m=n+1 \\ m \neq i}}^j \frac{|\langle \mathbf{h}_n, \mathbf{h}_m \rangle|^2}{\|\mathbf{h}_n\|^2 \|\mathbf{h}_m\|^2} \|\mathbf{h}_n\|^2 \|\mathbf{h}_m\|^2 + \sum_{\substack{n=1 \\ n \neq i}}^j \|\mathbf{h}_n\|^2} \right. \\ & \quad \left. \middle| \|\mathbf{h}_s\|^2 > u_k, \forall s \in \mathcal{S} \right] \end{aligned}$$

Now, we have a concave function of the form $-1/x$ inside the expectation. Accordingly, using Jensen inequality for concave functions, we obtain that

$$\begin{aligned} & \mathbb{E} [\text{tr}(\mathbf{R}) | \|\mathbf{h}_s\|^2 > u_k, \forall s \in \mathcal{S}] \\ & \leq r - (j-1)^2 u_k^2 \left(\mathbb{E} \left[\sum_{\substack{n=1 \\ n \neq i}}^j (\|\mathbf{h}_n\|^2)^2 + 2 \sum_{\substack{n=1 \\ n \neq i}}^j \sum_{\substack{m=n+1 \\ m \neq i}}^j \frac{|\langle \mathbf{h}_n, \mathbf{h}_m \rangle|^2}{\|\mathbf{h}_n\|^2 \|\mathbf{h}_m\|^2} \|\mathbf{h}_n\|^2 \|\mathbf{h}_m\|^2 \right. \right. \\ & \quad \left. \left. + \sum_{\substack{n=1 \\ n \neq i}}^j \|\mathbf{h}_n\|^2 \middle| \|\mathbf{h}_s\|^2 > u_k, \forall s \in \mathcal{S} \right] \right)^{-1} \\ & = r - (j-1)^2 u_k^2 \left(\sum_{\substack{n=1 \\ n \neq i}}^j \mathbb{E} \left[(\|\mathbf{h}_n\|^2)^2 \middle| \|\mathbf{h}_n\|^2 > u_k \right] \right. \\ & \quad \left. + 2 \sum_{\substack{n=1 \\ n \neq i}}^j \sum_{\substack{m=n+1 \\ m \neq i}}^j \mathbb{E} \left[\frac{|\langle \mathbf{h}_n, \mathbf{h}_m \rangle|^2}{\|\mathbf{h}_n\|^2 \|\mathbf{h}_m\|^2} \middle| \|\mathbf{h}_s\|^2 > u_k, \forall s \in \mathcal{S} \right] \right. \\ & \quad \left. \cdot \mathbb{E} [\|\mathbf{h}_n\|^2 | \|\mathbf{h}_n\|^2 > u_k] \mathbb{E} [\|\mathbf{h}_m\|^2 | \|\mathbf{h}_m\|^2 > u_k] + \sum_{\substack{n=1 \\ n \neq i}}^j \mathbb{E} [\|\mathbf{h}_n\|^2 | \|\mathbf{h}_n\|^2 > u_k] \right)^{-1} \end{aligned}$$

where the last equality follows from the linearity of the expectation and since $\frac{\langle \mathbf{h}_n, \mathbf{h}_m \rangle^2}{\|\mathbf{h}_n\|^2 \|\mathbf{h}_m\|^2}$, which is the angle between two independent vectors, \mathbf{h}_m and \mathbf{h}_n , is independent of the vectors' norms. Moreover, we can now remove the conditioning on the norm when taking the expectation of the angle. Accordingly, an upper bound can be evaluated by computing

the expectations in the denominator as follows.

$$\begin{aligned}
& r - (j-1)^2 u_k^2 \left(\sum_{\substack{n=1 \\ n \neq i}}^j \mathbb{E} \left[(\|\mathbf{h}_n\|^2)^2 \mid \|\mathbf{h}_n\|^2 > u_k \right] \right. \\
& \quad + 2 \sum_{\substack{n=1 \\ n \neq i}}^j \sum_{\substack{m=n+1 \\ m \neq i}}^j \mathbb{E} \left[\frac{|\langle \mathbf{h}_n, \mathbf{h}_m \rangle|^2}{\|\mathbf{h}_n\|^2 \|\mathbf{h}_m\|^2} \right] \mathbb{E} [\|\mathbf{h}_n\|^2 \mid \|\mathbf{h}_n\|^2 > u_k] \mathbb{E} [\|\mathbf{h}_m\|^2 \mid \|\mathbf{h}_m\|^2 > u_k] \\
& \quad \left. + \sum_{\substack{n=1 \\ n \neq i}}^j \mathbb{E} [\|\mathbf{h}_n\|^2 \mid \|\mathbf{h}_n\|^2 > u_k] \right)^{-1} \\
& \stackrel{(a)}{=} r - (j-1)^2 u_k^2 \\
& \quad \cdot \left((j-1)(u_k^2 + 2a_{\{K,r\}} u_k + 2a_{\{K,r\}}^2) + j(j-1) \frac{1}{r} (u_k + a_{\{K,r\}})^2 + (j-1)(u_k + a_{\{K,r\}}) \right)^{-1} \\
& = r - \frac{(j-1)u_k^2}{\left(1 + \frac{j}{r}\right) (u_k + a_{\{K,r\}})^2 + a_{\{K,r\}}(a_{\{K,r\}} + 1) + u_k},
\end{aligned}$$

where (a) follows since the limit distribution of the channel norm tail is exponentially distributed with rate parameter $1/a_{\{K,r\}}$ given that it is above high threshold. Namely, $\|\mathbf{h}_n\|^2 \mid \|\mathbf{h}_n\|^2 > u_k \sim \text{Exp}(1/a_{\{K,r\}})$, [38]. Thus, $\mathbb{E} \left[(\|\mathbf{h}_n\|^2)^2 \mid \|\mathbf{h}_n\|^2 > u_k \right]$ can be interpreted as a second moment of exponential random variable. Similar to Section 4, by [24, Lemma 3.2], the angle has the same distribution as that of the minimum of $r-1$ independent uniform $[0, 1]$ random variables (i.e., with CDF $1 - (1 - \alpha)^{r-1}$, $0 \leq \alpha \leq 1$). The expectations of the norms, again, follow from the EVT. Details are in Corollary 1, Section 7. \square

6.2 Threshold-based MMSE Lower Bound

To completely characterize the performance of the suggested threshold-based algorithm under MMSE decoding, we proceed to derive a corresponding lower bound. To this end, the following claims will be useful. The proofs are deferred to Section 7.

Claim 4. *Let \mathbf{H} be a complex Gaussian matrix with i.i.d. entries. Then,*

- (i) $\mathbf{R}^{-1} = (\mathbf{H}\mathbf{H}^\dagger + I)$ is unitary invariant. In particular, \mathbf{R} can be decomposed as $\mathbf{U}\mathbf{\Lambda}\mathbf{U}^\dagger$, where \mathbf{U} is a unitary matrix, independent of the diagonal matrix $\mathbf{\Lambda}$.
- (ii) The property above holds conditioned on all norms of the columns \mathbf{h}_i of \mathbf{H} being above a threshold u . In particular, conditioned on $\|\mathbf{h}_i\|^2 > u$, $U\mathbf{h}_i$ and \mathbf{h}_i have the same distribution.

Claim 5 (E.g., [3]). *For $s \geq 2$, we have $\Gamma(s, x) \geq e^{-x}(1+x)^{s-1}$.*

Claim 6. Let $\mathbf{x} \sim \chi_{2(r-j+1)}^2$ and let $\mathbf{y} \sim \chi_{2(j-1)}^2$, independent of \mathbf{x} , for some integer $1 < j \leq r$. Then,

$$E[\log(1 + \mathbf{x}) | \mathbf{x} + \mathbf{y} > u] > \left(\frac{\Gamma(r)\Gamma(r-j+1, u/2)}{\Gamma(r, u/2)\Gamma(r-j+1)} + \frac{e^{-u/2}u^{r-1}}{2^{r-1}\Gamma(r, u/2)} \right) \log(u) \\ + \frac{e^{-u/2}u^{r-1}}{2^{r-1}\Gamma(r, u/2)} (\psi(r-j+1) - \psi(r)) + e \frac{\Gamma(r)\Gamma(r-j, 1+u/2)}{\Gamma(r, u/2)\Gamma(r-j+1)},$$

where $\psi(x) = \frac{d}{dx} \ln \Gamma(x)$ is the Digamma function.

To understand Claim 6, note that $\Gamma(s, x) = (s-1)\Gamma(s-1, x) + x^{s-1}e^{-x}$. Hence, it is not hard to show that

$$\lim_{u \rightarrow \infty} \frac{\Gamma(r)\Gamma(r-j+1, u/2)}{\Gamma(r, u/2)\Gamma(r-j+1)} = 1.$$

Moreover, using Claim 5 above, one can also show that

$$0 \leq \frac{e^{-u/2}u^{r-1}}{2^{r-1}\Gamma(r, u/2)} \leq 1.$$

Hence, the importance of Claim 6 is in showing that $E[\log(1 + \mathbf{x}) | \mathbf{x} + \mathbf{y} > u_k] = \Theta(\log u_k)$. Similar to the upper bound, since $u_k = \Theta(\log K)$, the scaling law of $\Theta(\log \log K)$ will result.

To conclude, a lower bound on the performance of our threshold-based algorithm with MMSE receiver is as follows. For simplicity of the presentation, we assume $P = 1$.

Lemma 6. For sufficiently large K , the expected sum capacity under the threshold-based algorithm and MMSE decoding satisfies the following lower bound.

$$E[C(u_k)] > \sum_{j=2}^r \frac{k^j e^{-k}}{j!} j \left[\left(\frac{\Gamma(r)\Gamma(r-j+1, u_k/2)}{\Gamma(r, u_k/2)\Gamma(r-j+1)} + e^{-u_k/2} \frac{u_k^{r-1}}{2^{r-1}\Gamma(r, u_k/2)} \right) \log(u_k) \right. \\ \left. + e^{-u_k/2} \frac{u_k^{r-1}}{2^{r-1}\Gamma(r, u_k/2)} (\psi(r-j+1) - \psi(r)) + e \frac{\Gamma(r)\Gamma(r-j, 1+u_k/2)}{\Gamma(r, u_k/2)\Gamma(r-j+1)} \right].$$

Proof. We assume $1 < j \leq r$ users begin their transmission simultaneously and let \mathcal{S} denote the set of channels with norm greater than threshold. Note that when only one user passed the threshold, while its capacity is easy to compute, as it is the single-user MISO capacity, within this bound it is negligible as it is multiplied by the probability (under the Poisson distribution) that only one user passed the threshold. Hence, it is omitted for simplicity.

In this case, the capacity of stream i under MMSE receiver satisfies the following lower

bound.

$$\begin{aligned}
\mathbb{E}[C_i(u_k)] &= \mathbb{E} \left[\log \left(1 + P \mathbf{h}_i^\dagger \mathbf{R} \mathbf{h}_i \right) \middle| \|\mathbf{h}_s\|^2 > u_k, \forall s \in \mathcal{S} \right] \\
&\stackrel{(a)}{=} \mathbb{E} \left[\log \left(1 + P \sum_{n=1}^r \lambda_n(\mathbf{R}) |(U^\dagger \mathbf{h}_i)_n|^2 \right) \middle| \|\mathbf{h}_s\|^2 > u_k, \forall s \in \mathcal{S} \right] \\
&\stackrel{(b)}{=} \mathbb{E} \left[\log \left(1 + P \sum_{n=1}^r \frac{|(U^\dagger \mathbf{h}_i)_n|^2}{\lambda_n(\mathbf{R}^{-1})} \right) \middle| \|\mathbf{h}_s\|^2 > u_k, \forall s \in \mathcal{S} \right] \\
&\stackrel{(c)}{=} \mathbb{E} \left[\log \left(1 + P \left(\sum_{n=1}^{r-j+1} |(U^\dagger \mathbf{h}_i)_n|^2 + \sum_{n=r-j+2}^r \frac{|(U^\dagger \mathbf{h}_i)_n|^2}{\lambda_n(\mathbf{R}^{-1})} \right) \right) \middle| \|\mathbf{h}_s\|^2 > u_k, \forall s \in \mathcal{S} \right] \\
&\stackrel{(d)}{>} \mathbb{E} \left[\log \left(1 + P \sum_{n=1}^{r-j+1} |(U^\dagger \mathbf{h}_i)_n|^2 \right) \middle| \|\mathbf{h}_s\|^2 > u_k, \forall s \in \mathcal{S} \right] \\
&\stackrel{(e)}{=} \mathbb{E} \left[\log \left(1 + P \sum_{n=1}^{r-j+1} |(\mathbf{h}_i)_n|^2 \right) \middle| \|\mathbf{h}_s\|^2 > u_k, \forall s \in \mathcal{S} \right] \\
&= \mathbb{E} \left[\log \left(1 + P \sum_{n=1}^{r-j+1} |(\mathbf{h}_i)_n|^2 \right) \middle| \|\mathbf{h}_i\|^2 > u_k \right]
\end{aligned}$$

In the above chain of inequalities, (a) is since by Claim 4, there is a unitary matrix \mathbf{U} such that $\mathbf{R} = \mathbf{U} \mathbf{\Lambda} \mathbf{U}^\dagger$ with $\mathbf{\Lambda} = \text{diag}(\lambda_1, \dots, \lambda_r)$. As a result, we have the following quadric form:

$$\mathbf{h}^\dagger \mathbf{R} \mathbf{h} = \mathbf{h}^\dagger \mathbf{U} \mathbf{\Lambda} \mathbf{U}^\dagger \mathbf{h} = \sum_{n=1}^r \lambda_n(\mathbf{R}) |(U^\dagger \mathbf{h})_n|^2.$$

(b) is since the eigenvalues of \mathbf{R} are the reciprocals of those of \mathbf{R}^{-1} . (c) and (d) follow since, first, the dimensions of $\mathbf{H}_{(-i)} \mathbf{H}_{(-i)}^\dagger$ is $r \times r$ and its rank is $j - 1$. Thus, $r - j + 1$ of the eigenvalues of \mathbf{R}^{-1} (corresponding to the zero eigenvalues of $\mathbf{H}_{(-i)} \mathbf{H}_{(-i)}^\dagger$) are equal to one. Then, as $\mathbf{H}_{(-i)} \mathbf{H}_{(-i)}^\dagger$ is positive semidefinite, the non-zero eigenvalues are non negative. In fact, the eigenvalues of $\mathbf{H}_{(-i)} \mathbf{H}_{(-i)}^\dagger + I$ which are not unity, are relatively large as all columns of \mathbf{H} are above a threshold. (e) is by Claim 4 (ii).

Now, setting $\mathbf{x} = \sum_{n=1}^{r-j+1} |(\mathbf{h}_i)_n|^2$ and $\mathbf{x} + \mathbf{y} = \|\mathbf{h}_i\|^2$, Claim 6 completes the proof. \square

In Figure 11 we simulate the expected capacity of the threshold-based scheduling scheme, with MMSE-receiver and compare the simulation results to the upper and lower capacity bounds given in Lemma 5 and Lemma 6, respectively.

In Figure 12 we compare the MMSE receiver lower bound (dot-dashed line) and the ZF receiver lower bound (dashed line). As expected the MMSE achieves better performance when the threshold is lower, which corresponds to a lower SNR, and further, to a lower idle slot probability. On the other hand, as the threshold gets higher, which translates to high SNR, the ZF yields same results as MMSE. From this observation, since the MMSE receiver requires lower threshold to achieve higher sum-rate, we comprehend that the MMSE receiver is preferable to the ZF receiver, both in terms of sum-rate and idle slot probability, yet, still has a linear decoding complexity.

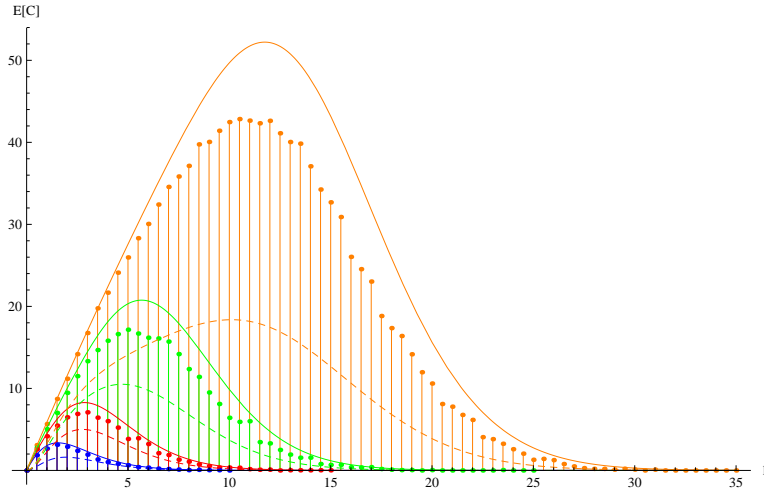


Figure 11: MMSE bounds. Bars are simulation results, while the solid and dashed lines represent upper and lower bound results respectively. Expected capacity under a single threshold algorithm and $K = 300$. The threshold u_k is set such that k users exceed it on average. Bars are the capacity under the threshold based scheme simulation results under MMSE receiver, while the solid and dashed lines represent the upper and lower bounds, respectively. The orange (upper), green (2nd from above), red (3rd from above) and blue (lower) lobes are for $r = 16, 8, 4$ and 2 receive antennas, respectively. Note that the optimal k is smaller than r .

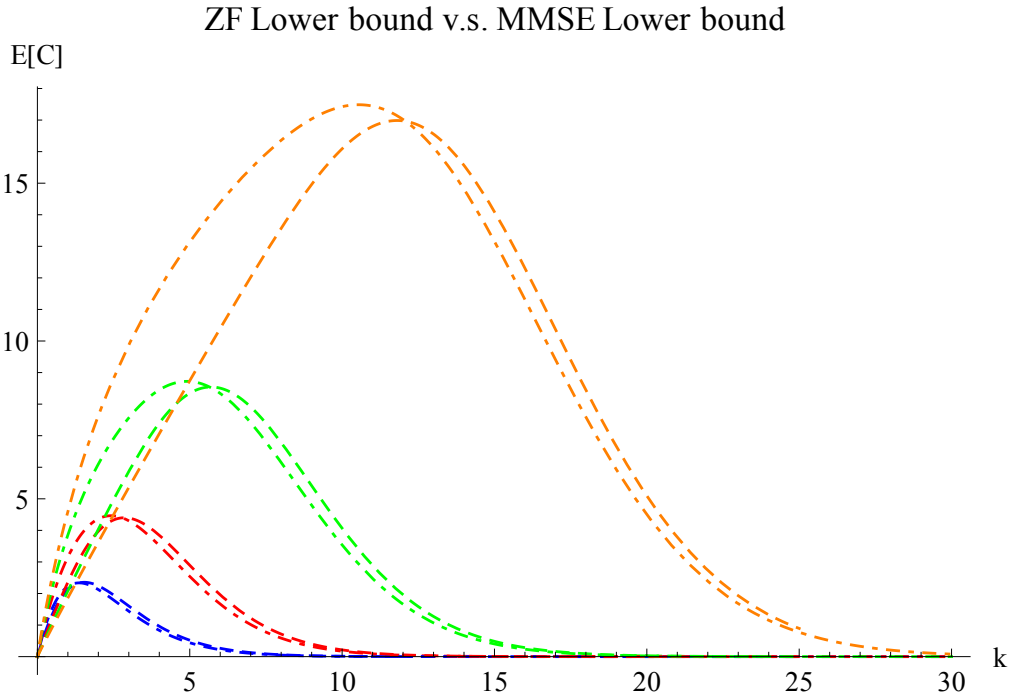


Figure 12: A comparison between the lower bound under an MMSE receiver (dot-dashed) and the lower bound under the ZF (dashed) receiver. The orange (upper), green (2nd from above), red (3rd from above) and blue (lower) lobes are for $r = 16, 8, 4$ and 2 receive antennas, respectively. Note that since one should choose k for best results, the MMSE lower bound predicts better results, achieved for a smaller k per r (the number of receive antennas).

7 Proofs

The methods discussed in the previous sections are based on a common baseline procedure. First, given that the norm threshold was exceeded, we wish to get a handle on the capacity distribution. Then, we wish to express the rate at which users exceed the threshold, in order to understand how likely is that a given number of users exceed a certain threshold. Finally, a threshold is estimated. This threshold is set according to the fraction of users which are required to exceed it on average. In this paper, the threshold is set on the channel vector norm, either directly or after projecting it on the null-space of the already chosen users. Note that we used a similar approach to analyze the expected rate, when the channel capacity is approximately Gaussian in [29]. In this section, we discuss the following problems directly for the problem at hand.

7.1 Threshold Arrival Rate and the Capacity Tail Distribution

Once a threshold is set, it is important to evaluate both the distribution of the number of users which exceed it as well as the conditional distribution of the norm given that the threshold was exceeded. Herein, we utilize the Point Process Approximation [42] and its specific usage for threshold arrival rates in the *single user case* [29] in order to derive these distributions for the problem at hand.

Assume that $\mathbf{x}_1, \dots, \mathbf{x}_n$ is a sequence of i.i.d. random variables with a distribution function $F(x)$, such that $F(x)$ is in the domain of attraction of some GEV distribution G , with normalizing constants a_n and b_n . We construct a sequence of points P_1, P_2, \dots on $[0, 1] \times \mathbb{R}$ by

$$P_n = \left\{ \left(\frac{i}{n}, \frac{\mathbf{x}_i - b_n}{a_n} \right), i = 1, 2, \dots, n \right\},$$

and examine the limit process, as $n \rightarrow \infty$. Consider P_n on the set $[0, 1] \times (b_l + \epsilon, \infty)$, where $\epsilon > 0$. By [42], $P_n \rightarrow P$ as $n \rightarrow \infty$, where P is a non-homogeneous Poisson process with intensity density $\lambda(t, x) = (1 + \xi x)_+^{-\frac{1}{\xi} - 1}$. x is the sample value, and t is the index of occurrence. In fact, in the i.i.d. case, the process intensity density $\lambda(t, x)$ is independent of t .

Let $\Lambda(B)$ be the expected number of points in the set B . $\Lambda(B)$ can be obtained by integrating the intensity of the Poisson process over B , That is $\Lambda(B) = \int_{b \in B} \lambda(b) db$. As we are interested in sets of the form $B_v = [0, 1] \times (v, \infty)$, where $v > b_l$ (threshold exceedance), we have $\Lambda(B_v) = (1 + \xi v)_+^{-1/\xi}$, where a_+ denotes $\max\{0, a\}$ (e.g., [29]). That is, the number of users whose channel norms exceed a threshold can be modeled by a Poisson process, with parameter $\Lambda(B_v)$. Note that for $\xi \rightarrow 0$, as in the case of the χ^2 distribution, we have $\Lambda(B_v) \rightarrow e^{-v}$, hence setting a threshold $\log K - \log k$ results in a per-user arrival rate of $\frac{k}{K}$, and, as a result, a total arrival rate of k .

To compute the conditional distribution, we proceed similar to [29]. For any fixed $v > b_l$,

let $u_n(v) = a_n v + b_n$, and let $x > 0$. Then

$$\begin{aligned} \Pr(\mathbf{x}_i > a_n x + u_n(v) | \mathbf{x}_i > u_n(v)) & \\ \rightarrow \Pr(P(t) > x + v | P(t) > v) & \\ = \frac{\Lambda(B_{x+v})}{\Lambda(B_v)} & \\ = \left[\left(1 + \xi \frac{x}{1 + \xi v} \right)_+ \right]^{-1/\xi} & \end{aligned}$$

where $P_n(t)$ and $P(t)$ are the corresponding excess value $\frac{\mathbf{x}_i - b_n}{a_n}$ at index t , and the corresponding excess value at time t in the limit process, respectively. Namely, the result is a generalized Pareto distribution, $GPD(a_n \sigma_v, \xi)$.

Note that for the χ^2 distribution, $\xi \rightarrow 0$, and we have

$$\Pr(\mathbf{x} - u_n(v) \leq \alpha | \mathbf{x} - u_n(v) > 0) = 1 - e^{-\frac{\alpha}{a_n}}$$

for all $\alpha \geq 0$. That is, the tail distribution can be approximated using an exponential distribution with rate $\lambda = 1/a_n$. As a result, taking the expected value, we obtain the following corollary.

Corollary 1. *Given a random complex Gaussian vector, and a threshold such that k users out of K exceed it on average, then*

$$E \left[\|\mathbf{h}\|^2 \mid \|\mathbf{h}\|^2 > u_k \right] = u_k + a_{\{K,r\}},$$

where $a_{\{K,r\}}$ is given in (4).

7.2 Threshold Estimation

Let u_k be a threshold such that only the k users with the strongest channel norm $\|\mathbf{h}_i\|^2$ will exceed it on average. Since $\|\mathbf{h}_i\|^2$ follows χ_{2r}^2 distribution, u_k can be easily estimated using the Inverse-Gamma function. That is,

$$u_k = 2Q^{-1}(r, k/K).$$

Note, however, that the expression above does not give any intuition on the actual threshold value, or, more importantly, how it scales with K for fixed k . Yet, note that the threshold u_k is closely related to the normalizing constant $b_{\{K,r\}}$, since both aim to capture the last quantiles of the ancestor distribution. The exact relation can be obtain using the Point process approximation. Specifically, the exceedance rate for the χ^2 -distribution is

$$\Lambda(u_k) = e^{-\frac{u_k - b_{\{K,r\}}}{a_{\{K,r\}}}}.$$

Accordingly, choosing $u_k = -a_{\{K,r\}} \log k + b_{\{K,r\}}$ gives a rate of k in total. Thus, letting $a_{\{K,r\}}$ and $b_{\{K,r\}}$ to be set according to (4) and (5), respectively, u_k is set. Now, to see the scaling law, note that $b_{\{K,r\}}$ in (5) converges to b_K in (3), hence $u_k = O(\log K)$. Figure 13 depicts the above convergence result.

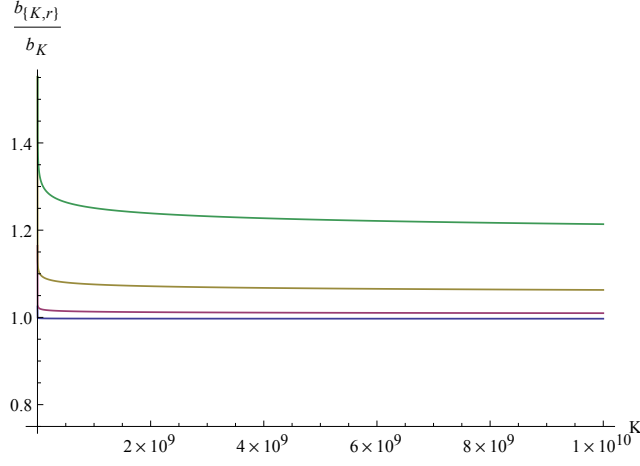


Figure 13: The ratio between the normalizing constant $b_{\{K,r\}}$ in (5) and the value in (3). The curves are plotted for $r = 16, 8, 4$ and 2 , top to bottom.

7.3 Proof of Claim 2

We wish to solve the following definite integral:

$$(r-1) \int_0^1 (1-\alpha)^{r-2} \log(1+Pu\alpha) d\alpha.$$

We first make the substitution $x = (1-\alpha)$. As a result, we obtain the following integral:

$$(r-1) \int_0^1 x^{r-2} \log(1+Pu(1-x)) dx.$$

Now, using integration by parts, we have

$$(r-1) \int_0^1 x^{r-2} \log(1+Pu(1-x)) dx = x^{r-1} \log(1+Pu(1-x)) \Big|_0^1 + \int_0^1 \frac{Pux^{r-1}}{1+Pu(1-x)} dx.$$

First, note that

$$x^{r-1} \log(1+Pu(1-x)) \Big|_0^1 = 0.$$

Now, performing a polynomial long division, the term inside the integral can be expressed as

$$\frac{Pux^{r-1}}{1+Pu(1-x)} = -\sum_{i=0}^{r-2} \left(\frac{1+Pu}{Pu}\right)^i x^{r-2-i} + \frac{(1+Pu)^{r-1}}{(Pu)^{r-2}(1+Pu(1-x))}.$$

Finally, we exchange the integration with the (finite) summation, then integrate each term in the sum according to dx . We have:

$$\begin{aligned}
& \int_0^1 \frac{Pux^{r-1}}{1+Pu(1-x)} dx \\
&= - \sum_{i=0}^{r-2} \left(\frac{1+Pu}{Pu} \right)^i \frac{1}{r-1-i} x^{r-1-i} \Big|_0^1 - \left(\frac{1+Pu}{Pu} \right)^{r-1} \log(1+Pu(1-x)) \Big|_0^1 \\
&= \left(\frac{1+Pu}{Pu} \right)^{r-1} \log(1+Pu) - \sum_{i=0}^{r-2} \left(\frac{1+Pu}{Pu} \right)^i \frac{1}{r-1-i}.
\end{aligned}$$

Thus, Claim 2 follows.

7.4 Proof of Claim 3

It can be shown by the total law of expectation, that the entries of the channel vector remain zero, given that the channel norm is greater than a threshold, as follows.

$$\begin{aligned}
\mathbb{E} \left[h_{i,n} \mid \|\mathbf{h}_i\|^2 > u_k \right] &= \mathbb{E} \left[h_{i,n} \mid \sum_{n=1}^r |h_{i,n}|^2 > u_k \right] \\
&= \mathbb{E} \left[\mathbb{E} \left[h_{i,n} \mid \sum_{n=1}^r |h_{i,n}|^2 > u_k, \sum_{\substack{m=1, \\ m \neq n}}^r |h_{i,m}|^2 = \tilde{u} \right] \mid \sum_{n=1}^r |h_{i,n}|^2 > u_k \right] \\
&= \mathbb{E} \left[\underbrace{\mathbb{E} \left[h_{i,n} \mid |h_{i,n}|^2 > u_k - \tilde{u} \right]}_{(*)} \mid \sum_{n=1}^r |h_{i,n}|^2 > u_k \right]
\end{aligned}$$

Since $h_{i,n}$ is complex Gaussian random variable, the inner expectation (*) can be decomposed to a real and an imaginary part as

$$\begin{aligned}
\mathbb{E} \left[h_{i,n} \mid |h_{i,n}|^2 > u_k - \tilde{u} \right] &= \mathbb{E} \left[a + ib \mid a^2 + b^2 > u_k - \tilde{u} \right] \\
&= \mathbb{E} \left[a \mid a^2 + b^2 > u_k - \tilde{u} \right] + i \mathbb{E} \left[b \mid a^2 + b^2 > u_k - \tilde{u} \right]
\end{aligned}$$

To ease notation, let us denote $\tilde{u} \doteq \sqrt{u_k - \tilde{u} - b^2}$. Focusing on the real part, we use the total expectation law again to obtain:

$$\begin{aligned}
\mathbb{E} \left[a \mid a^2 + b^2 > u_k - \tilde{u} \right] &= \mathbb{E} \left[\mathbb{E} \left[a \mid a^2 > u_k - \tilde{u} - b^2, b^2 \right] \mid a^2 + b^2 > u_k - \tilde{u} \right] \\
&= \mathbb{E} \left[\mathbb{E} \left[a \mid |a| > \tilde{u}, b^2 \right] \mid a^2 + b^2 > u_k - \tilde{u} \right] \\
&= \mathbb{E} \left[\underbrace{\mathbb{E} \left[\text{sign}(a) |a| \mid |a| > \tilde{u}, b^2 \right]}_{(**)} \mid a^2 + b^2 > u_k - \tilde{u} \right].
\end{aligned}$$

Now, we show that the sign of a is independent of the amplitude $|a|$ and b^2 .

$$\begin{aligned}
\Pr\left(\text{sign}(a) = -1 \mid |a| > \tilde{u}, b^2\right) &= \Pr\left(a < 0 \mid |a| > \tilde{u}, b^2\right) \\
&= \frac{\Pr\left(a < 0, |a| > \tilde{u}, b^2\right)}{\Pr\left(|a| > \tilde{u}, b^2\right)} \\
&= \frac{\Pr\left(a < -\tilde{u}, b^2\right)}{\Pr\left(a < -\tilde{u}, b^2\right) + \Pr\left(a > \tilde{u}, b^2\right)} \\
&= \frac{1}{2}.
\end{aligned}$$

Thus, the sign of a , the amplitude $|a|$ and b^2 are independent. Consequently, the inner expectation (***) is equal to:

$$\begin{aligned}
\mathbb{E}\left[\text{sign}(a) |a| \mid |a| > \tilde{u}, b^2\right] &= \mathbb{E}[\text{sign}(a)] \mathbb{E}[|a| \mid |a| > \tilde{u}, b^2] \\
&= 0.
\end{aligned}$$

From symmetry, same result can be obtained for the imaginary part. Thus, the vectors are still zero mean vectors.

However, the variance of the vector entries increase, given that the vector norm is greater than a threshold. Remember, by EVT [38], the tail is exponentially distributed with rate parameter $1/a_{\{K,r\}}$. Thus, it follows that

$$\begin{aligned}
u_k + a_{\{K,r\}} &\stackrel{(a)}{=} \mathbb{E}\left[\|\mathbf{h}_i\|^2 \mid \|\mathbf{h}_i\|^2 > u_k\right] \\
&\stackrel{(b)}{=} \sum_{n=1}^r \mathbb{E}\left[|h_{i,n}|^2 \mid \|\mathbf{h}_i\|^2 > u_k\right] \\
&\stackrel{(c)}{=} r \mathbb{E}\left[|h_{i,n}|^2 \mid \|\mathbf{h}_i\|^2 > u_k\right]
\end{aligned}$$

where (a) is the result of computing the expected norm of an i.i.d. complex normal random vector, given that it exceeded a threshold u_k . (b) follows from the linearity of expectation operator. (c) is since the elements of \mathbf{h}_i are identically distributed. We point out that choosing vectors with norm greater than a threshold increase the variance of the entries to $(u_k + a_{\{K,r\}})/r$.

Similar to the entries conditional expectation, it can be shown that the matrix entries are still uncorrelated in pairs. Namely,

$$\begin{aligned}
&\mathbb{E}\left[h_{i,n}^* h_{i,m} \mid \|\mathbf{h}_i\|^2 > u_k\right] \\
&= \mathbb{E}\left[h_{i,n}^* h_{i,m} \mid \sum_{n=1}^r |h_{i,n}|^2 > u_k\right] \\
&= \mathbb{E}\left[\mathbb{E}\left[h_{i,n}^* h_{i,m} \mid \sum_{n=1}^r |h_{i,n}|^2 > u_k, \sum_{\substack{m=1 \\ m \neq n}}^r |h_{i,m}|^2 = \tilde{u}\right] \mid \sum_{n=1}^r |h_{i,n}|^2 > u_k\right] \\
&= \mathbb{E}\left[\underbrace{\mathbb{E}\left[h_{i,n}^* h_{i,m} \mid |h_{i,n}|^2 > u_k - \tilde{u}\right]}_{(*)} \mid \sum_{n=1}^r |h_{i,n}|^2 > u_k\right]
\end{aligned}$$

Similar to the method above, we decompose $h_{i,n}^*$ to its real and imaginary part. Thus, the inner expectation $(*)$ is

$$\begin{aligned}
\mathbb{E} \left[h_{i,n}^* h_{i,m} \mid |h_{i,n}|^2 > u_k - \tilde{u} \right] \\
&= \mathbb{E} \left[ah_{i,m} - ibh_{i,m} \mid a^2 + b^2 > u_k - \tilde{u} \right] \\
&= \mathbb{E} \left[ah_{i,m} \mid a^2 + b^2 > u_k - \tilde{u} \right] - i \mathbb{E} \left[bh_{i,m} \mid a^2 + b^2 > u_k - \tilde{u} \right]
\end{aligned}$$

Using the total expectation law on the real part of the expectation, we have

$$\begin{aligned}
\mathbb{E} \left[ah_{i,m} \mid a^2 + b^2 > u_k - \tilde{u} \right] \\
&= \mathbb{E} \left[\mathbb{E} \left[ah_{i,m} \mid a^2 > u_k - \tilde{u} - b^2, b^2 \right] \mid a^2 + b^2 > u_k - \tilde{u} \right] \\
&= \mathbb{E} \left[\underbrace{\mathbb{E} \left[\text{sign}(a) |a| h_{i,m} \mid |a| > \tilde{u}, b^2 \right]}_{(**)} \mid a^2 + b^2 > u_k - \tilde{u} \right].
\end{aligned}$$

Now, similar to the above method, let us show that the sign of a is independent of $|a|$ and $h_{i,m}$.

$$\begin{aligned}
\Pr \left(\text{sign}(a) = -1 \mid |a| > \tilde{u}, b^2, h_{i,m} \right) &= \Pr \left(a < 0 \mid |a| > \tilde{u}, b^2, h_{i,m} \right) \\
&= \frac{\Pr \left(a < 0, |a| > \tilde{u}, b^2, h_{i,m} \right)}{\Pr \left(|a| > \tilde{u}, b^2, h_{i,m} \right)} \\
&= \frac{\Pr \left(a < -\tilde{u}, b^2, h_{i,m} \right)}{\Pr \left(a < -\tilde{u}, b^2, h_{i,m} \right) + \Pr \left(a > \tilde{u}, b^2, h_{i,m} \right)} \\
&= \frac{1}{2} = \Pr(a < 0).
\end{aligned}$$

Thus, the inner expectation $(**)$ can be expressed as

$$\begin{aligned}
\mathbb{E} \left[\text{sign}(a) |a| h_{i,m} \mid |a| > \tilde{u}, b^2 \right] &= \mathbb{E} \left[\text{sign}(a) \right] \mathbb{E} \left[|a| h_{i,m} \mid |a| > \tilde{u}, b^2 \right] \\
&= 0.
\end{aligned}$$

From symmetry, same result can be obtained for the imaginary part. Thus, given that the norm is greater than a threshold, the vector entries sill are uncorrelated. Thus, Claim 3 follows.

7.5 Proof of Claim 4

A Hermitian random matrix is unitary invariant if the joint distribution of its entries does not change under unitary transformation, namely, $\mathbf{H} \sim U\mathbf{H}$ for any unitary matrix U . It is well known that a Gaussian matrix is unitary invariant (e.g., [1]). It is not hard to see that $\mathbf{H}\mathbf{H}^\dagger \sim U\mathbf{H}\mathbf{H}^\dagger U^\dagger$. That is, the Wishart matrix is also unitary invariant. Similarly, as $UIU^\dagger = I$, $(\mathbf{H}\mathbf{H}^\dagger + I) \sim U(\mathbf{H}\mathbf{H}^\dagger + I)U^\dagger$.

Since $(\mathbf{H}\mathbf{H}^\dagger + I)$ is unitary invariant, by [2, Lemma 2.6], there is a decomposition such that $(\mathbf{H}\mathbf{H}^\dagger + I) = \mathbf{U}\tilde{\mathbf{\Lambda}}\mathbf{U}^\dagger$, \mathbf{U} being unitary and independent of $\tilde{\mathbf{\Lambda}}$, hence $(\mathbf{H}\mathbf{H}^\dagger + I)^{-1} = \mathbf{U}\tilde{\mathbf{\Lambda}}^{-1}\mathbf{U}^\dagger$ and part (i) follows with $\mathbf{\Lambda} = \tilde{\mathbf{\Lambda}}^{-1}$. Note that if we are only interested in the decomposition, and the independence between the unitary matrix and the eigenvalues is not required (as is the case in the lower bound below), the proof is simpler since \mathbf{R} is Hermitian.

For part (ii), note that if $\mathbf{h} \sim U\mathbf{h}$, then $\mathbf{h} \mid \|\mathbf{h}_i\|^2 > u \sim U\mathbf{h} \mid \|\mathbf{h}_i\|^2 > u$. This is since the unitary transform does not change the vector norm, hence the set of instances $h \in \mathbb{C}^r$ with $\|h\|^2 > u$ is the same as those with $\|Uh\|^2 > u$. The rest follows in the same manner.

7.6 Proof of Claim 5

First, note that,

$$\Gamma(s, x) = \int_x^\infty \tau^{s-1} e^{-\tau} d\tau = e^{-x} \int_0^\infty (t+x)^{s-1} e^{-t} dt = e^{-x} \mathbf{E}[(T+x)^{s-1}],$$

where $T \sim \exp(1)$.

Accordingly, since $(t+x)^{s-1}$ is convex in t for the corresponding s , we apply Jensen's inequality to the r.h.s. and note that $\mathbf{E}[T] = 1$, proving the bound.

7.7 Proof of Claim 6

We wish to bound the following expectation, when $\mathbf{x} \sim \chi_{2(r-j+1)}^2$ and $\mathbf{y} \sim \chi_{2(j-1)}^2$, independent of \mathbf{x} :

$$\begin{aligned} E[\log(1 + \mathbf{x}) \mid \mathbf{x} + \mathbf{y} > u] &= \frac{1}{\Pr(\mathbf{x} + \mathbf{y} > u)} \\ &\left[\int_{x=0}^u \int_{y=u-x}^\infty \log(1+x) f_{\mathbf{x}}(x) f_{\mathbf{y}}(y) dy dx + \int_{x=u}^\infty \int_{y=0}^\infty \log(1+x) f_{\mathbf{x}}(x) f_{\mathbf{y}}(y) dy dx \right]. \end{aligned}$$

Performing integration on y , we have the following.

$$\begin{aligned} E[\log(1+x) \mid \mathbf{x} + \mathbf{y} > u] &= \frac{1}{\Pr(\mathbf{x} + \mathbf{y} > u)} \left[\underbrace{\int_{x=0}^u \frac{\Gamma(j-1, (u-x)/2)}{\Gamma(j-1)} \log(1+x) f_{\mathbf{x}}(x) dx}_{I_2(x)} + \underbrace{\int_{x=u}^\infty \log(1+x) f_{\mathbf{x}}(x) dx}_{I_1(x)} \right] \end{aligned} \quad (12)$$

where $\Gamma(s, x) = \int_x^\infty t^{s-1} e^{-t} dt$ is the upper incomplete Gamma function. Further, note that the complement CDF of the $\chi_{2(j-1)}^2$ -distribution is $\Pr(\mathbf{y} > u-x) = \frac{\Gamma(j-1, (u-x)/2)}{\Gamma(j-1)}$.

Accordingly, to evaluate (12), we need to evaluate both $I_1(x)$ and $I_2(x)$. We begin with integration by parts on $I_1(x)$, where the anti-derivative is $f_{\mathbf{x}}(x)$. We have

$$\begin{aligned} I_1(x) &= \log(1+x) \int_{x=u}^\infty f_{\mathbf{x}}(x) dx - \int_{x=u}^\infty \frac{\int f_{\mathbf{x}}(x) dx}{1+x} dx \\ &= \log(1+x) \left(-\frac{\Gamma(r-j+1, x/2)}{\Gamma(r-j+1)} \right) \Big|_{x=u}^\infty + \frac{1}{\Gamma(r-j+1)} \int_{x=u}^\infty \frac{\Gamma(r-j+1, x/2)}{1+x} dx, \end{aligned}$$

where the last equality follows since $\int f_{\mathbf{x}}(x)dx = \int \frac{x^{r-j}e^{-x/2}}{2^{r-j+1}\Gamma(r-j+1)}dx = -\frac{\Gamma(r-j+1,x/2)}{\Gamma(r-j+1)}$. Now, to bound the above expression, we restrict our attention to $1 < j \leq r$. Since $\lim_{x \rightarrow \infty} \log(1+x)\Gamma(s, x/2) = 0$, utilizing Claim 5, we have

$$\begin{aligned}
I_1(x) &\geq \frac{\Gamma(r-j+1, u/2)}{\Gamma(r-j+1)} \log(1+u) + \frac{1}{\Gamma(r-j+1)} \int_{x=u}^{\infty} \frac{e^{-x/2}(1+x/2)^{r-j}}{1+x} dx \\
&> \frac{\Gamma(r-j+1, u/2)}{\Gamma(r-j+1)} \log(1+u) + \frac{1}{\Gamma(r-j+1)} \int_{x=u}^{\infty} \frac{e^{-x/2}(1+x/2)^{r-j}}{2+x} dx \\
&= \frac{\Gamma(r-j+1, u/2)}{\Gamma(r-j+1)} \log(1+u) + \frac{1}{2\Gamma(r-j+1)} \int_{x=u}^{\infty} e^{-x/2}(1+x/2)^{r-j-1} dx \\
&= \frac{\Gamma(r-j+1, u/2)}{\Gamma(r-j+1)} \log(1+u) + \frac{e}{\Gamma(r-j+1)} \int_{z=1+u/2}^{\infty} e^{-z} z^{r-j-1} dz \\
&= \frac{\Gamma(r-j+1, u/2)}{\Gamma(r-j+1)} \log(1+u) + \frac{e}{\Gamma(r-j+1)} \Gamma(r-j, 1+u/2).
\end{aligned}$$

Next, let us address $I_2(x)$. Again, using Claim 5, we have

$$\begin{aligned}
I_2(x) &\geq \frac{1}{\Gamma(j-1)} \int_{x=0}^u e^{-\frac{u-x}{2}} \left(1 + \frac{u-x}{2}\right)^{j-2} \log(1+x) f_{\mathbf{x}}(x) dx \\
&= \frac{1}{\Gamma(j-1)} \int_{x=0}^u e^{-\frac{u-x}{2}} \left(1 + \frac{u-x}{2}\right)^{j-2} \log(1+x) \frac{x^{r-j} e^{-x/2}}{2^{r-j+1} \Gamma(r-j+1)} dx \\
&= \frac{e^{-u/2}}{2^{r-j+1} \Gamma(r-j+1) \Gamma(j-1)} \int_{x=0}^u \left(1 + \frac{u-x}{2}\right)^{j-2} x^{r-j} \log(1+x) dx \\
&= \frac{e^{-u/2}}{2^{j-2} 2^{r-j+1} \Gamma(r-j+1) \Gamma(j-1)} \int_{x=0}^u (2+u-x)^{j-2} x^{r-j} \log(1+x) dx \\
&> \frac{e^{-u/2}}{2^{r-1} \Gamma(r-j+1) \Gamma(j-1)} \int_{x=0}^u (u-x)^{j-2} x^{r-j} \log(1+x) dx \\
&= \frac{e^{-u/2} u^{r-2}}{2^{r-1} \Gamma(r-j+1) \Gamma(j-1)} \int_{x=0}^u \left(1 - \frac{x}{u}\right)^{j-2} \left(\frac{x}{u}\right)^{r-j} \log(1+x) dx
\end{aligned}$$

Let $z = x/u$. Accordingly, we have

$$\begin{aligned}
I_2(x) &> \frac{e^{-u/2} u^{r-1}}{2^{r-1} \Gamma(r-j+1) \Gamma(j-1)} \int_{z=0}^1 (1-z)^{j-2} z^{r-j} \log(1+uz) dz \\
&\geq \frac{e^{-u/2} u^{r-1} \beta(r-j+1, j-1)}{2^{r-1} \Gamma(r-j+1) \Gamma(j-1)} \int_{z=0}^1 \frac{1}{\beta(r-j+1, j-1)} (1-z)^{j-2} z^{r-j} \log(uz) dz \\
&= \frac{e^{-u/2} u^{r-1} \beta(r-j+1, j-1)}{2^{r-1} \Gamma(r-j+1) \Gamma(j-1)} \left[\log(u) \int_{z=0}^1 \frac{1}{\beta(r-j+1, j-1)} (1-z)^{j-2} z^{r-j} dz \right. \\
&\quad \left. + \int_{z=0}^1 \frac{1}{\beta(r-j+1, j-1)} (1-z)^{j-2} z^{r-j} \log(z) dz \right]
\end{aligned}$$

where $\beta(r-j+1, j-1) = \frac{\Gamma(r-j+1)\Gamma(j-1)}{\Gamma(r)}$ is the Beta function. Note that while $\log(z) \rightarrow -\infty$ as $z \rightarrow 0$, the integral converges as this is the mean of $\log(Z)$ when Z has a Beta distribution.

Accordingly, we have

$$I_2(x) > \frac{e^{-u/2}u^{r-1}}{2^{r-1}\Gamma(r)} [\log(u) + \psi(r - j + 1) - \psi(r)].$$

To complete the proof, remember that $Pr(\mathbf{x} + \mathbf{y} > u) = \frac{\Gamma(r, u/2)}{\Gamma(r)}$. Thus, we have

$$E[\log(1 + x)|\mathbf{x} + \mathbf{y} > u] > \frac{\Gamma(r)}{\Gamma(r, u/2)} \left(\frac{e^{-u/2}u^{r-1}}{2^{r-1}\Gamma(r)} [\log(u) + \psi(r - j + 1) - \psi(r)] \right. \\ \left. + \frac{\Gamma(r - j + 1, u/2)}{\Gamma(r - j + 1)} \log(1 + u) + e^{-\frac{\Gamma(r - j, 1 + u/2)}{\Gamma(r - j + 1)}} \right).$$

8 Conclusion

In this paper, we suggested a distributed multiuser scheduling algorithm which utilizes the multiuser diversity and achieves the optimal capacity scaling laws (for large number of users). Specifically, we offered threshold-based algorithms, and characterized the scaling law of the expected capacity under linear decoding, e.g., ZF, ZF-SIC and MMSE. To support the results, we provided both tractable analysis which gave insightful results as well as simulations which showed tightness even for moderate number of users. We concluded that the distributed algorithm achieves the optimal scaling laws, i.e., $\Theta(r \log \log K)$.

References

- [1] Telatar, E., “Capacity of Multi-antenna Gaussian Channels,” in *European transactions on telecommunications*, vol 10, 1999, pp.585–595.
- [2] Tulino, Antonia Maria and Verdú, Sergio, “Random matrix theory and wireless communications,” *Now Publishers Inc*, vol 1, 2004.
- [3] <http://math.stackexchange.com/questions/129170/are-there-well-known-lower-bounds-for-the-upper> MATHEMATICS, 2012.
- [4] Bai, Zhaojun and Golub, Gene H., “Bounds for the trace of the inverse and the determinant of symmetric positive definite matrices,” in *Annals of Numerical Mathematics*, vol 4, 1996, pp. 29–38.
- [5] Johnson, Norman L and Kotz, Samuel and Balakrishnan, N, “Distributions in Statistics: Continuous Univariate Distributions: Vol.: 2”, *Houghton Mifflin New York*, 1970.
- [6] Kim, Namshik and Lee, Yusung and Park, Hyuncheol, “Performance analysis of MIMO system with linear MMSE receiver”, in *Wireless Communications, IEEE Transactions on*, vol 7, 2008, pp. 4474–4478.
- [7] Li, Ping and Paul, Debashis and Narasimhan, Ravi and Cioffi, John, “On the distribution of SINR for the MMSE MIMO receiver and performance analysis,” in *Information Theory, IEEE Transactions on*, vol 52, 2006, pp. 271–286.

- [8] Gartner, ME and Bolcskei, H., “Multiuser space-time/frequency code design,” in *Information Theory, 2006 IEEE International Symposium on*, 2006, pp. 2819–2823.
- [9] Qin, X. and Berry, R.A., “Distributed power allocation and scheduling for parallel channel wireless networks,” in *Wireless Networks*, vol 14, 2008, pp. 601–613, Kluwer Academic Publishers.
- [10] Aruba Networks, “802.11ac In-Depth”, available at http://www.arubanetworks.com/wp-content/uploads/WP_80211acTechnologyCh13.pdf, 2012.
- [11] R. Knopp and P. Humblet, “Information capacity and power control in single-cell multiuser communications,” in *IEEE International Conference on Communications, Seattle*, vol. 1, 1995, pp. 331–335.
- [12] R. Gozali, R. Buehrer, and B. Woerner, “The impact of multiuser diversity on space-time block coding,” *Communications Letters, IEEE*, vol. 7, no. 5, pp. 213–215, 2003.
- [13] J. Kim, S. Park, J. Lee, J. Lee, and H. Jung, “A scheduling algorithm combined with zero-forcing beamforming for a multiuser MIMO wireless system,” in *IEEE Vehicular Technology Conference*, vol. 1, 2005, pp. 211–215.
- [14] M. Airy, S. Shakkattai, and R. Heath Jr, “Spatially greedy scheduling in multi-user MIMO wireless systems,” in *the Thirty-Seventh Asilomar Conference on Signals, Systems and Computers*, vol. 1. IEEE, 2003, pp. 982–986.
- [15] C. Swannack, E. Uysal-Biyikoglu, and G. Wornell, “Low complexity multiuser scheduling for maximizing throughput in the MIMO broadcast channel,” in *Proc. Allerton Conf. Communications, Control and Computing*, 2004.
- [16] G. Primolevo, O. Simeone, and U. Spagnolini, “Channel aware scheduling for broadcast MIMO systems with orthogonal linear precoding and fairness constraints,” in *IEEE International Conference on Communications*, vol. 4, 2005, pp. 2749–2753.
- [17] T. Yoo, N. Jindal, and A. Goldsmith, “Finite-rate feedback MIMO broadcast channels with a large number of users,” in *Information Theory, 2006 IEEE International Symposium on*. IEEE, 2006, pp. 1214–1218.
- [18] T. Yoo and A. Goldsmith, “On the optimality of multiantenna broadcast scheduling using zero-forcing beamforming,” *Selected Areas in Communications, IEEE Journal on*, vol. 24, no. 3, pp. 528–541, 2006.
- [19] H. Weingarten, Y. Steinberg, and S. Shamai, “The capacity region of the gaussian multiple-input multiple-output broadcast channel,” *Information Theory, IEEE Transactions on*, vol. 52, no. 9, pp. 3936–3964, 2006.
- [20] G. Caire, “MIMO downlink joint processing and scheduling: a survey of classical and recent results,” in *Proc. Workshop on Information Theory and Its Applications*, 2006.
- [21] B. Hassibi and M. Sharif, “Fundamental limits in MIMO broadcast channels,” *Selected Areas in Communications, IEEE Journal on*, vol. 25, no. 7, pp. 1333–1344, 2007.

- [22] M. Sharif and B. Hassibi, “A comparison of time-sharing, dpc, and beamforming for MIMO broadcast channels with many users,” *Communications, IEEE Transactions on*, vol. 55, no. 1, pp. 11–15, 2007.
- [23] Z. Shen, R. Chen, J. Andrews, R. Heath, and B. Evans, “Low complexity user selection algorithms for multiuser MIMO systems with block diagonalization,” *Signal Processing, IEEE Transactions on*, vol. 54, no. 9, pp. 3658–3663, 2006.
- [24] K. Jagannathan, S. Borst, P. Whiting, and E. Modiano, “Efficient scheduling of multi-user multi-antenna systems,” in *Modeling and Optimization in Mobile, Ad Hoc and Wireless Networks, 2006 4th International Symposium on*. IEEE, 2006, pp. 1–8.
- [25] —, “Scheduling of multi-antenna broadcast systems with heterogeneous users,” *Selected Areas in Communications, IEEE Journal on*, vol. 25, no. 7, pp. 1424–1434, 2007.
- [26] X. Qin and R. Berry, “Exploiting multiuser diversity for medium access control in wireless networks,” in *INFOCOM 2003. Twenty-Second Annual Joint Conference of the IEEE Computer and Communications. IEEE Societies*, vol. 2. IEEE, 2003, pp. 1084–1094.
- [27] —, “Distributed approaches for exploiting multiuser diversity in wireless networks,” *Information Theory, IEEE Transactions on*, vol. 52, no. 2, pp. 392–413, 2006.
- [28] K. Bai and J. Zhang, “Opportunistic multichannel aloha: distributed multiaccess control scheme for OFDMA wireless networks,” *Vehicular Technology, IEEE Transactions on*, vol. 55, no. 3, pp. 848–855, 2006.
- [29] D. Kampeas, A. Cohen, and O. Gurewitz, “Opportunistic scheduling in heterogeneous networks: Distributed algorithms and system capacity,” *arXiv preprint arXiv:1202.0119*, 2012.
- [30] J. Kampeas, A. Cohen, and O. Gurewitz, “Capacity of distributed opportunistic scheduling in heterogeneous networks,” in *Proceedings of the Annual Allerton Conference on Communication Control and Computing*, 2012.
- [31] J. Choi and F. Adachi, “User selection criteria for multiuser systems with optimal and suboptimal LR based detectors,” *Signal Processing, IEEE Transactions on*, vol. 58, no. 10, pp. 5463–5468, 2010.
- [32] J. Laneman and G. Wornell, “Distributed space-time-coded protocols for exploiting cooperative diversity in wireless networks,” *Information Theory, IEEE Transactions on*, vol. 49, no. 10, pp. 2415–2425, 2003.
- [33] R. Zakhour and S. Hanly, “Min-max fair coordinated beamforming via large system analysis,” *IEEE International Symposium on Information Theory Proceedings*, pp. 1896–1900, 2011.
- [34] L. Wang, C. Chiu, C. Yeh, and C. Li, “Coverage enhancement for OFDM-based spatial multiplexing systems by scheduling,” in *IEEE Wireless Communications and Networking Conference, WCNC*. IEEE, 2007, pp. 1439–1443.

- [35] M. Pun, V. Koivunen, and H. Poor, “Opportunistic scheduling and beamforming for MIMO-SDMA downlink systems with linear combining,” in *IEEE 18th International Symposium on Personal, Indoor and Mobile Radio Communications*, 2007, pp. 1–6.
- [36] W. Choi and J. Andrews, “The capacity gain from intercell scheduling in multi-antenna systems,” *Wireless Communications, IEEE Transactions on*, vol. 7, no. 2, pp. 714–725, 2008.
- [37] L. De Haan and A. Ferreira, *Extreme value theory: an introduction*. Springer Verlag, 2006.
- [38] M. Leadbetter, *Extremes and Related Properties of Random Sequences and Processes*. Springer-Verlag, N.Y, 1983.
- [39] P. Embrechts, C. Klüppelberg, and T. Mikosch, *Modelling extremal events: for insurance and finance*. Springer, 2011, vol. 33.
- [40] D. Tse and P. Viswanath, *Fundamentals of wireless communication*. Cambridge university press, 2005.
- [41] A. Janssen, J. Van Leeuwen, and B. Zwart, “Gaussian expansions and bounds for the poisson distribution applied to the erlang b formula,” *Advances in Applied Probability*, vol. 40, no. 1, pp. 122–143, 2008.
- [42] R. Smith, “Extreme value analysis of environmental time series: an application to trend detection in ground-level ozone,” *Statistical Science*, vol. 4, no. 4, pp. 367–377, 1989.